# Turning lakes into river gauges using the LakeFlow algorithm

Ryan M Riggs[1], George Henry Allen[2], Craig B Brinkerhoff[3], Md. Safat Sikder[4], and Jida Wang[4]

[1]Texas A&M University
[2]Virginia Tech
[3]University of Massachusetts Amherst
[4]Kansas State University

April 4, 2023

**Abstract**

Rivers and lakes are intrinsically connected waterbodies yet they are rarely used to hydrologically constrain one another with remote sensing. Here we begin to bridge the gap between river and lake hydrology with the introduction of the LakeFlow algorithm. LakeFlow uses river-lake mass conservation and observations from the Surface Water and Ocean Topography (SWOT) satellite to provide river discharge estimates of lake and reservoir inflows and outflows. We test LakeFlow performance at three lakes using a synthetic SWOT dataset containing the maximum measurement errors defined by the mission science requirements, and we include modeled lateral inflow and lake evaporation data to further constrain the mass balance. We find that LakeFlow produces promising discharge estimates (median Nash-Sutcliffe efficiency=0.88, relative bias=14%). LakeFlow can inform water resources management by providing global lake inflow and outflow estimates, highlighting a path for recognizing rivers and lakes as an interconnected system.

# Turning lakes into river gauges using the LakeFlow algorithm

Ryan M. Riggs[1], George H. Allen[2], Craig B. Brinkerhoff[3], Md. Safat Sikder[4], Jida Wang[4]
(1)Department of Geography, Texas A&M University, College Station, TX, USA, (2)Department of Geosciences, Virginia Polytechnic Institute and State University, Blacksburg, VA, USA, (3)Department of Civil and Environmental Engineering, University of Massachusetts Amherst, Amherst, MA, USA, (4)Department of Geography and Geospatial Sciences, Kansas State University, Manhattan, KS, USA.

**Key points:**

1. LakeFlow is a new algorithm that uses SWOT satellite data to estimate river inflow and outflow at lakes via mass conservation.
2. Applying LakeFlow to three sample lake systems shows promising performance for estimating lake inflows and outflows (median NSE = 0.88).
3. Including modeled estimates of non SWOT-observed evaporation and tributary inflows can further improve LakeFlow discharge estimates.

**Abstract**

Rivers and lakes are intrinsically connected waterbodies yet they are rarely used to hydrologically constrain one another with remote sensing. Here we begin to bridge the gap between river and lake hydrology with the introduction of the LakeFlow algorithm. LakeFlow uses river-lake mass conservation and observations from the Surface Water and Ocean Topography (SWOT) satellite to provide river discharge estimates of lake and reservoir inflows and outflows. We test LakeFlow performance at three lakes using a synthetic SWOT dataset containing the maximum measurement errors defined by the mission science requirements, and we include modeled lateral inflow and lake evaporation data to further constrain the mass balance. We find that LakeFlow produces promising discharge estimates (median Nash-Sutcliffe efficiency=0.88, relative bias=14%). LakeFlow can inform water resources management by providing global lake inflow and outflow estimates, highlighting a path for recognizing rivers and lakes as an interconnected system.

**Plain language summary**

Effective water resource management depends on our ability to monitor and understand lake and reservoir inflows and outflows. Satellite remote sensing of lakes and rivers has become increasingly important for water management but little work has been done to estimate streamflow at river-lake interfaces. Here we present the LakeFlow algorithm that leverages satellite observations of lakes and rivers to estimate streamflow at lake inflows and outflows. We test LakeFlow at three U.S. lakes in Georgia, Arizona and Kansas, and find that it provides promising estimates of streamflow at river-lake boundaries. LakeFlow provides valuable insights into river-lake streamflow dynamics, which can inform water management decisions and is a step forward in the integration of river and lake studies.

## 1. Introduction

Rivers and lakes serve as vital sources of freshwater for ecosystems and civilizations worldwide (Everard and Powell, 2002; Macklin and Lewin, 2015; Yevjevich, 1992). While rivers and lakes are often treated as separate systems in large-scale remote sensing studies, their hydrologies are intimately related such that hydrologic changes in one water body type can be used to constrain the hydrology of an adjacent water body of a different type (Vörösmarty et al., 2000). For example, the relationship between inflow and outflow of a natural lake or human-made reservoir (hereinafter collectively referred to as a “lake” unless otherwise stated) can control the lake’s volumetric water storage and water surface elevation. Natural lakes located along river networks can attenuate local discharge downstream and actively managed reservoirs can significantly affect downstream flow regime by altering the natural timing and quantity of river discharge (Doll et al., 2009; Wang et al., 2017; Yang et al., 2022). Reservoir inflow and outflow dynamics are key for modeling reservoir operations, which can be difficult to simulate from water mass balance alone, especially at the continental to global scale (Cohen et al., 2014; Harrigan et al., 2020).

At these large scales, understanding of the hydrologic interplay between rivers and lakes has largely been developed through the analysis of streamflow gauges located on lake inflows and outflows (i.e., the rivers flowing into and out of a lake), as well as lake-level gauges (Batalla et al., 2004; Shiklomanov and Lammers, 2009; Yang et al., 2008). Unfortunately, most of Earth’s lakes do not have publicly available gauge data and those that do are primarily located on large lakes or in a few geographically isolated regions (Brazil National Water Agency, 2022; Do et al., 2018; Gudmundsson et al., 2018; U.S. Geological Survey, 2022). This lack of observational data limits our understanding of how impoundments impact surface water flows and has motivated the development of alternative techniques for supplementing river and lake gauge observations.

Satellite remote sensing is uniquely capable of providing observation-based discharge estimates in near-real time and at the global scale (Smith, 1997). Although remote sensing of discharge (RSQ) has been performed using a variety of satellite data and techniques (Gleason and Durand, 2020), much of the recent focus has been in preparation for the recently launched Surface Water and Ocean Topography (SWOT) mission (Biancamaria et al., 2016). Though SWOT cannot directly observe river discharge, it can potentially provide unprecedented cotemporal measurements of river area, elevation, width, and slope for all rivers within the SWOT River Database (SWORD) (Altenau et al., 2021). The SWOT mission will also produce discharge estimates calculated by combining cotemporal SWOT observations with flow laws (e.g. hydraulic geometry, Manning's equation), mass conservation principles, and a priori estimates of non-SWOT-observable flow-law parameters (FLP) such as frictional resistance (Manning's n) and bathymetry (Brinkerhoff et al., 2020; Durand et al., 2014). These SWOT discharge estimates will be practically produced using the Confluence program which houses several different RSQ algorithms (Durand et al., 2023). SWOT RSQ algorithms are sensitive to FLP estimates (Durand et al., 2016) which are provided by the SWORD of Science (SoS) database for all rivers in SWORD (Brinkerhoff et al., 2020). SoS priors of Manning's n and bathymetry are developed using *in situ* measurements that are then paired with river attributes such as mean width, allowing for mean width alone to provide prior estimates of these FLPs. Although SWOT discharge is expected to improve our understanding of global river discharge (Pavelsky et al., 2014), existing SWOT RSQ algorithms do not leverage SWOT observations of lakes into their workflow, which could improve performance.

In lakes, SWOT can observe lake surface area and elevation, which together can be combined to estimate volumetric storage change (Busker et al., 2019; Crétaux et al., 2011; Gao, 2015; Zhao and Gao, 2019). Storage change estimates are valuable for understanding seasonal and long-term trends in water availability and usage (Cooley et al., 2021; Keys and Scott, 2018; Ryan et al., 2020). Storage change fluctuations also influence downstream river discharge

(Nickles and Beighley, 2021; Wang et al., 2013) but very few remote sensing applications consider lakes and rivers as an interconnected system (Gardner et al., 2019). The few remote sensing studies that do assess lakes and rivers together rely on modeled discharge and use satellite estimates of lake storage change to revise the modeled outflow discharge (Bonnema and Hossain, 2019; Yoon et al., 2016; Yoon and Beighley, 2015). This calibration only improves the difference between the inflow and outflow discharge, leaving the original bias in the modeled inflow (or outflow) discharge uncorrected (Bonnema et al., 2016b). However, the accuracies for both inflow and outflow discharge are important because together they provide key insights into human water management and the impact lakes have on river flow regime. Currently, SWOT RSQ algorithms have neither been assessed nor are specifically designed to run at river-lake boundaries (Bonnema et al., 2016a; Durand et al., 2016; Frasson et al., 2021).

To address these gaps in our ability to monitor the river-lake continuum, we develop LakeFlow, an algorithm which applies river-lake mass conservation to estimate both lake inflow and outflow discharge. Like other SWOT RSQ algorithms, LakeFlow relies on Manning’s equation and mass conservation (Feng et al., 2021; Hagemann et al., 2017) but also leverages additional SWOT observations of lake storage change to further constrain river discharge. In addition to discharge, LakeFlow estimates Manning’s n and bathymetry of lake inflow and outflow channels, which can be used to inform or improve other SWOT RSQ algorithms. LakeFlow could potentially be applied to the nearly 17 thousand SWOT observable lakes that are located along the SWORD network and have at least one inflow and one outflow reach that are observable from SWOT (Figure 1). In total, LakeFlow could possibly provide valuable insights into discharge dynamics at 19,380 inflow and 16,959 outflow reaches that are connected to

SWOT observable lakes. Ultimately, LakeFlow bridges the gap between lake storage and river discharge to improve SWOT discharge coverage and accuracy.

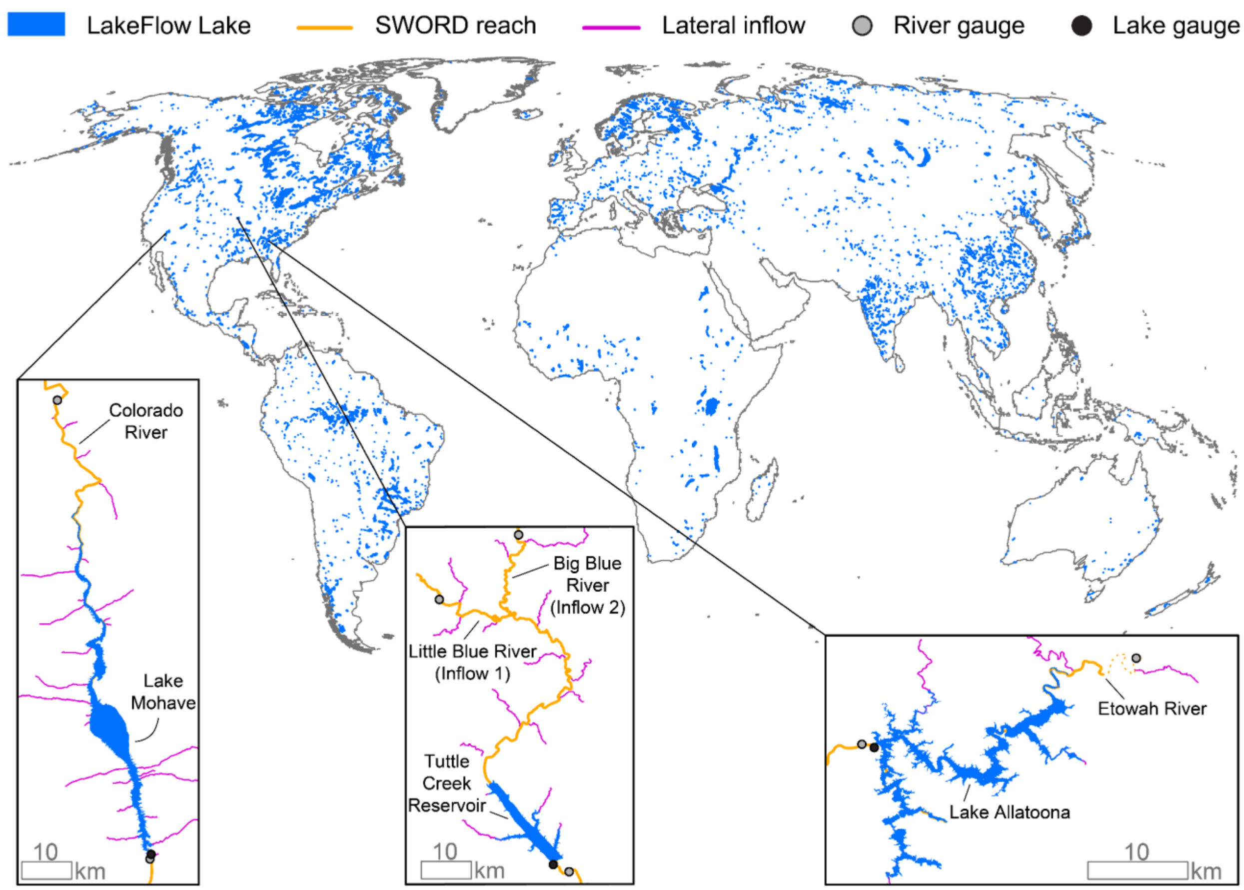


**Figure 1**. Global distribution of lakes suitable for LakeFlow implementation (N=16,610) with three sample lakes highlighted. Each of these lakes is observable by SWOT (Sheng et al., 2016) and contains at least one SWOT observable inflow and one SWOT observable outflow (Allen and Pavelsky, 2018; Altenau et al., 2021). Note the Lake Allatoona inflow gauge is located on the inflow mainstem (dashed orange line) but is located 7 km upstream of the SWORD reach (orange line).

## 2. Methods

### 2.1 LakeFlow algorithmic design

The LakeFlow algorithm uses SWOT observed river and lake variables to estimate discharge. LakeFlow uses the modified version of Manning's equation from Durand et al. (2014) to describe discharge dynamics for the inflow and outflow reaches,

$$Q = n^{-1}(A_0 + \delta A)^{5/3} W^{-2/3} S^{1/2}, \quad (1)$$

where $Q$ is discharge and $n$ is the frictional resistance of the river channel, referred to as Manning's n. $A_0$ represents the unobservable cross-sectional area that extends beyond the minimum observed water level, hereinafter referred to as bathymetry, $\delta A$ is the SWOT observable change in cross-sectional area, $W$ is river width, and $S$ is slope. LakeFlow leverages SWOT estimated lake storage change ($\delta V$) during the time period between two consecutive SWOT overpasses ($p$) to constrain inflow and outflow discharge based on mass conservation,

$$\delta V_p = \int_{t=0}^{p} \left( {n_i}^{-1}(A_{0i} + \delta A_i)^{5/3} {W_i}^{-2/3} {S_i}^{1/2} - {n_o}^{-1}(A_{0o} + \delta A_o)^{5/3} W_o^{-2/3} {S_o}^{1/2} + Q_l - E \right)_t. \quad (2)$$

Here $t$ represents any time during period $p$, $Q_l$ is lateral inflows from channels too small to been observed by SWOT, $E$ is lake evaporation, and all other variables are the same as eq. 1 with $i$ and $o$ denoting the variables of the SWOT observable inflow and outflow reaches, respectively (Figure 2). Simply put, LakeFlow assumes that lake storage change is equal to inflow minus outflow discharge while accounting for lateral inflows and evaporation. While SWOT provides estimates of lake storage change ($\delta V$), change in river cross-sectional area ($\delta A$), slope ($S$), and width ($W$), it does not observe Manning's n ($n$) or bathymetry ($A_0$) for the inflow and outflow reaches, leaving four unknown variables in eq. 2. Note that for simplicity, we only include one inflow reach and one outflow reach for eq. 2 but LakeFlow has the capability to be applied on lakes with multiple inflow and outflow reaches.

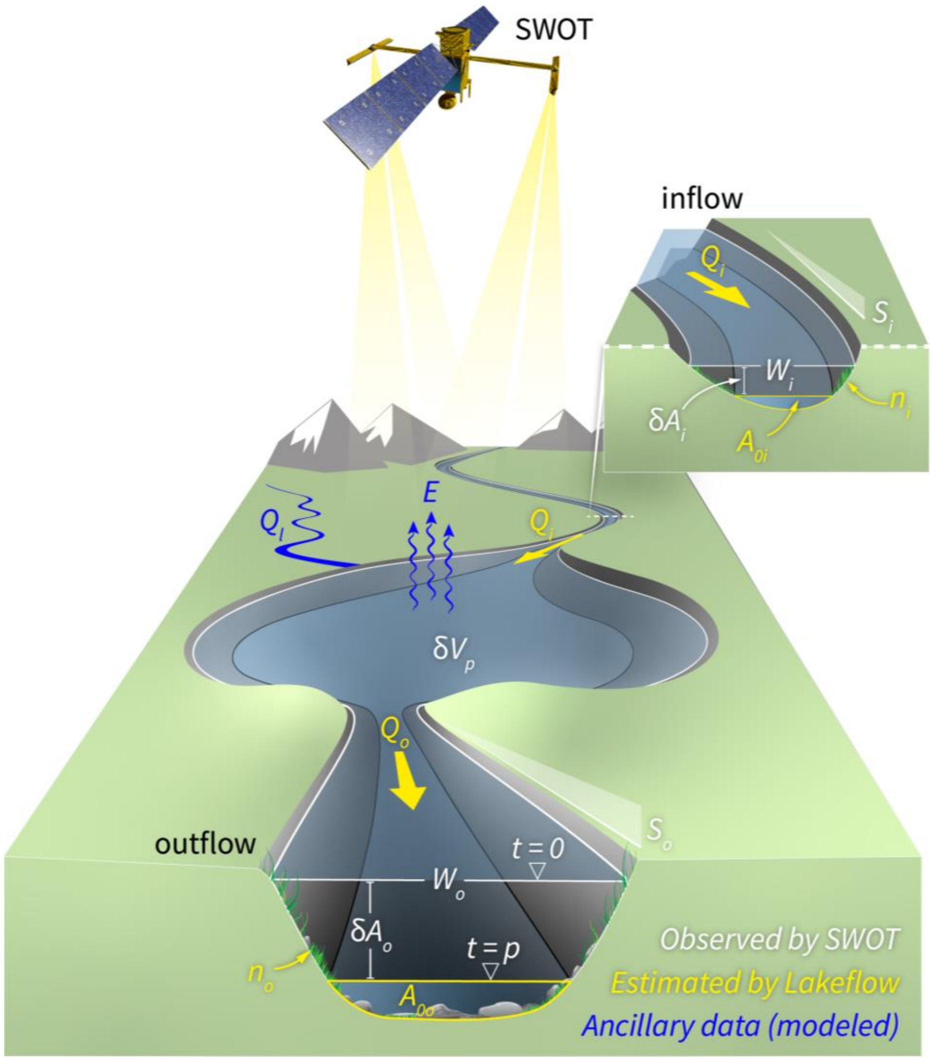


**Figure 2**. Conceptual diagram of the LakeFlow algorithm which uses repeat SWOT observations of lakes and rivers to estimate the inflows and outflows of lakes in cubic meters per second. See eq. 1 and 2 for variable definitions. Shown are two snapshots of a lake system corresponding to two SWOT overpasses (*t=0* and *t=p*). Note that time *p* corresponds to the minimum observed flow and that only SWOT observable variables are shown for *t=0*.

Like many other SWOT RSQ algorithms, LakeFlow struggles from parameter equifinality; there are roughly equal numbers of known and unknown parameters in eq. 2. Following the approach of Hagemann et al. (2017) and Brinkerhoff et al. (2022), we use

Bayesian inference to constrain the uncertainty in LakeFlow's unknown parameters ($n_i$, $A_{0i}$ , $n_o$, $A_{0o}$) given repeated SWOT observations. Bayesian approaches start from Bayes rule,

$$p(\Theta|x) = \frac{f(x|\Theta)p(\Theta)}{p(x)}, \quad (3)$$

where $\Theta$ is a set of unobserved SWOT parameters, $x$ is the SWOT observed data, $f(x|\Theta)$ is the sampling model where data are conditional on the parameters, and $p(\Theta)$is the joint prior distribution of the parameters. Thus, we are interested in approximating $p(\Theta|x)$, the posterior distribution. Bayesian inference aims to approximate the posterior distribution by assuming proportionality ( $p(\Theta|x) \propto f(x|\Theta)p(\Theta)$) and using Monte Carlo sampling. To implement the Bayesian inference, we log transform and scale Manning's equation to have integer coefficients,

$$6\, log\, Q = -6\, log\, n + 10\, log(A_0 + \delta A) - 4\, log\, W + 3\, log\, S. \quad (4)$$

To provide a likelihood equation, we rearrange eq. 4 to isolate the measured variables for both the inflow and outflow reaches,

$$4\, log\, W - 3\, log\, S = -6\, log\, n - 6\, logQ + 10\, log(A_0 + \delta A), \quad (5)$$

and the likelihood equation for river-lake mass conservation is,

$$\delta V - Q_l + E = exp(logQ_i) - exp(logQ_o). \quad (6)$$

The Bayesian approach requires prior estimates of all unknown parameters in eq. 2 which are taken from the SWOT SoS. In addition to estimates of Manning's n and bathymetry, the SoS provides gauge-constrained and unconstrained modeled estimates of mean flow and LakeFlow uses the gauge-constrained estimate, taken from the Global Reach-Level A Priori Discharge Estimates for SWOT (GRADES) model product (Lin et al., 2019). The Bayesian inference uses the Stan probabilistic programming language (Stan Development Team, 2023) to approximate the posterior distribution and provide estimates of all unknowns in eq. 2.

## 2.2 Datasets

We investigate the performance of LakeFlow in three sample lakes spanning a range of climate regions as seen in Figure 1: Lake Allatoona (humid); Lake Mohave (arid); and Tuttle Creek Reservoir (semi-arid). Lake Allatoona (area: 36 $km^2$) is a flood control reservoir along the Etowah River in northwestern Georgia. Lake Mohave (area: 99 $km^2$) is a hydropower reservoir on the Colorado River spanning the border of Arizona and Nevada. Tuttle Creek Reservoir (area: 43 $km^2$) is located in northeastern Kansas and is built to control floods on the Little Blue and Big Blue Rivers. These lakes each have a U.S. Geological Survey (USGS) gauge station on or near their SWOT observable inflow and outflow reaches as well as on the lakes themselves. Lake Allatoona and Lake Mohave each contain one inflow and one outflow reach and Tuttle Creek Reservoir has two inflow reaches.

Because SWOT data are not yet available, we generate a synthetic dataset of SWOT observable variables by utilizing gauge records from the USGS (U.S. Geological Survey, 2022), a Landsat-based water occurrence map (Pekel et al., 2016), and a priori channel attributes provided in SWORD. We then corrupt these data to produce SWOT-like observations by using the measurement errors defined by the mission science requirements and limit the number of observations to one observation per week corresponding to the approximate average overpass rate of SWOT over these lakes (Biancamaria et al., 2016). The synthetic dataset is developed using hydraulic principles and contains values of non SWOT observed Manning's n and bathymetry (see Supplemental Text S1 for details of the synthetic dataset). The historical time period of the synthetic dataset is determined by the availability of USGS gauge records, such that the measurements of the lake and its inflow and outflow must all overlap in time. As a result, the timespan ($p$ in eq. 2) for each of the three lakes is 10/01/2009 to 09/30/2014 for Lake Allatoona, 10/01/2008 to 09/30/2013 for Lake Mohave, and 10/01/2006 to 09/30/2011 for Tuttle Creek Reservoir.

Where the LakeFlow algorithm can run, lake storage change is predominantly governed by large-river inflows and outflows that are observable by SWOT, but lake storage change can also be influenced by other factors including inflow from groundwater runoff, small lateral streams (pink lines in Figure 1), and evaporation loss (Tayfur et al., 2007; Tian et al., 2022; Zhao et al., 2022). To study the impact of including these factors on LakeFlow's performance, we run two scenarios of LakeFlow: one that only includes SWOT-based observations and a second that includes SWOT observations and also ancillary datasets of lateral inflow and evaporation, represented by $Q_l$ and $E$ in eq. 2, respectively. We estimate lateral inflow using high-resolution simulated discharge from GRADES (Lin et al., 2019) and we estimate evaporation losses using modeled data from the Global Lake Evaporation Volume (GLEV) dataset (Zhao et al., 2022) (see Supplemental Text S2 for details of these ancillary datasets). We then assess LakeFlow's performance related to the ancillary datasets for each of the three study sites by comparing same-day LakeFlow estimated discharge with gauge discharge from the USGS and calculate Nash-Sutcliffe Efficiency (NSE), relative bias (rBias), normalized root-mean-square error (NRMSE), and mean absolute error (MAE) (Table S1). In addition to assessing discharge accuracy, we compare LakeFlow FLP estimates with the synthetic dataset's values of Manning's n and bathymetry. We further compare LakeFlow FLP estimates with the SoS prior estimates to assess LakeFlow's capabilities for informing other SWOT-based RSQ algorithms. The SoS FLPs are chosen for comparison as these are the default prior FLP estimates for SWOT RSQ algorithms (Durand et al., 2023) (see section 1 for more information).

## 3. Results

The results of the analysis, generated from synthetic SWOT data at the three test sites, indicate that the LakeFlow algorithm will be able to successfully estimate lake inflows and outflows from SWOT observations. In general, we find that LakeFlow estimated discharge skillfully resembles the gauge hydrograph for all of the inflow and outflow reaches (Figure 3). However, there is clear bias on some reaches, namely the Allatoona Lake Inflow and Tuttle Creek Reservoir Inflow 1. Even where there are biases present, LakeFlow captures flow variability for each of the reaches analyzed here as evidenced by a positive NSE for all reaches and a median NSE and NRMSE of 0.88 and 29.0%, respectively. While two reaches have relatively large rBias values, all of the other reaches have an absolute rBias less than 15% with a median rBias of 13.5%, indicating that on average, LakeFlow provides near-zero discharge estimates at river-lake interfaces.

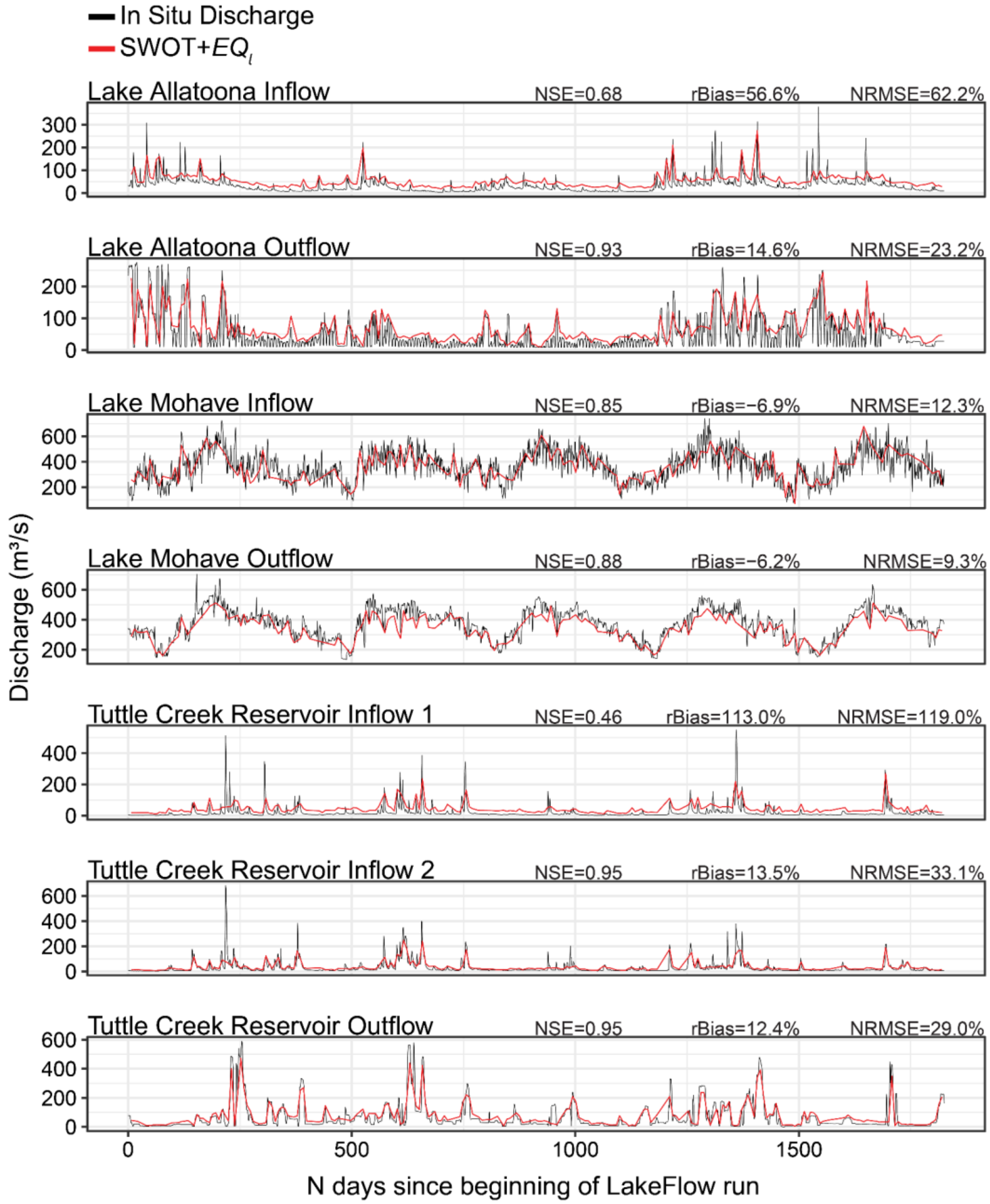


**Figure 3.** LakeFlow estimated discharge for all lake inflows and outflows compared to gauge records.

LakeFlow accurately estimates discharge dynamics across all seven study reaches (Figure 4a). Overall, LakeFlow discharge performance tends to modestly improve with the addition of the lateral inflow and evaporation ancillary datasets but does not tend to improve with the addition of only a single one of these datasets (Figure S1). This discrepancy is likely due to the inherent bias introduced when only including one of these ancillary terms. LakeFlow discharge mean absolute error (MAE) improves by 1.6% when both ancillary datasets are included compared to including neither. However, the bias marginally increases when both ancillary data are used but remains near-zero (Figure 4a). With and without the ancillary data, LakeFlow discharge for each study location correlates well with same-day gauge discharge observations with marginal overestimations and underestimations in low and high flows, respectively (Pearson correlation coefficient, $R$ ranges from 0.95 to 0.99).

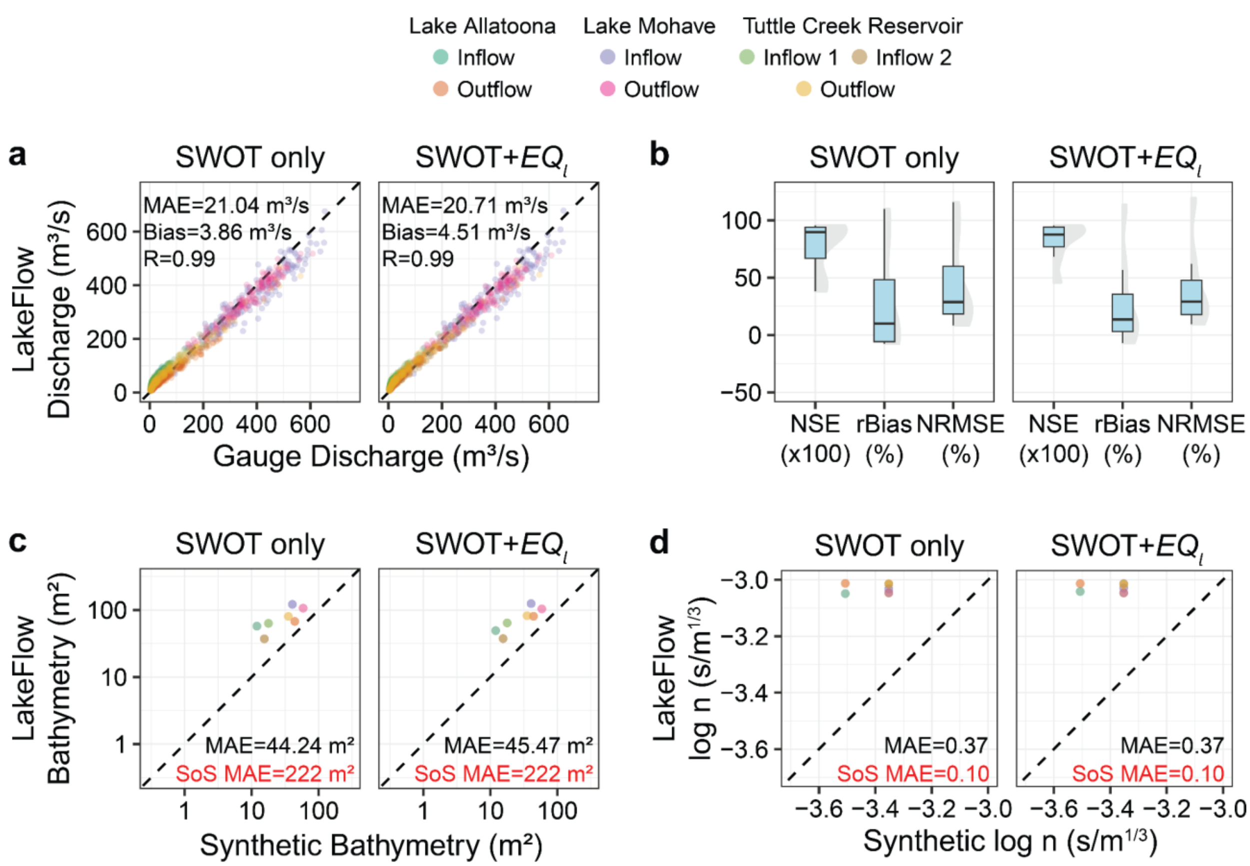


**Figure 4.** LakeFlow performance without ("SWOT only") and with ("SWOT+$EQ_l$") ancillary data. (a) Scatterplots of same-day gauge discharge vs. LakeFlow estimated discharge across all reaches. (b) Boxplots and half violin plots of LakeFlow discharge performance metrics across all

reaches: NSE (scaled by 100), rBias (%), and NRMSE (%). (c) Scatterplots of synthetic bathymetry vs. LakeFlow estimated bathymetry across all reaches. (d) Scatterplots of log synthetic Manning's n vs. log LakeFlow estimated Manning's n across all reaches.

Across all reaches, we find that discharge performance modestly improves with the addition of the ancillary data (Figure 4b). For example, the mean NSE and NRMSE improve by 4.8% and 6.7%, respectively, when including ancillary data. Conversely, there is a positive bias present in most reaches and the mean rBias is unaffected by the inclusion of the ancillary data. Nearly all of the metrics have a negatively skewed distribution, indicating that LakeFlow performs well on average but occasionally exhibits poor performance. In addition to estimating discharge, LakeFlow can estimate unobserved bathymetry ($A_0$) and Manning's n, with MAE values of 44 $m^2$ and 0.37 $s/m^{1/3}$ (log), respectively. Across all reaches and scenarios, LakeFlow MAE for bathymetry is on average 80% lower than the SoS MAE (Figure 4c) while LakeFlow estimated Manning's n values are marginally worse than the SoS (Figure 4d). LakeFlow tends to overestimate Manning's n values in the three test lakes, which may be related to bathymetry estimates having a positive bias. Bathymetric accuracy declines by 2.8% and Manning's n accuracy remains stable with the inclusion of the ancillary data.

## 4. Discussion

The LakeFlow algorithm can provide useful discharge estimates at river-lake interfaces and will enhance the SWOT mission's capabilities for monitoring surface water dynamics. We do not test LakeFlow in locations where other SWOT RSQ algorithms have been assessed, but our findings indicate that LakeFlow's discharge accuracy is comparable or better than other SWOT RSQ algorithms (Frasson et al., 2021), thus providing the capability to extend the SWOT discharge product to river-lake boundaries with no expected decline in accuracy. These discharge data can inform hydroelectric and water management decisions and improve our understanding of how reservoir dynamics affect the surrounding environment (Barnett and Pierce, 2008; Chadwick et al., 2021; Huang et al., 2019; Wang et al., 2018). Reservoir operations are particularly important in transboundary water basins where water management in upstream portions of the basin can lead to actual or perceived inequities in downstream water distribution (UNEP, 2016). However, LakeFlow inflow and outflow discharge estimates can potentially increase the transparency of reservoir management practices with implications for water management decisions within transboundary basins (Gleason and Hamdan, 2017).

In addition to discharge, LakeFlow's ability to accurately estimate Manning's n and bathymetry values could provide useful geomorphic insights near river-lake interfaces. Compared to the SoS, LakeFlow provides marginally worse Manning's n estimates but significantly more accurate bathymetric estimates. However, Manning's n values are inherently limited to a small range of 0.02-0.07 $s/m^{1/3}$ (Arcement and Schneider, 1989) whereas bathymetry varies widely globally. Since RSQ algorithms are sensitive to prior FLP estimates (Bonnema et al., 2016a; Durand et al., 2016; Tuozzolo et al., 2019), the more accurate LakeFlow bathymetries could improve the performance and efficiency of other RSQ algorithms near river-lake interfaces. Thus, there is potential to implement LakeFlow into the SWOT Confluence program (Durand et al., 2023) to inform other SWOT RSQ algorithms.

While LakeFlow is shown to perform well at the three study sites presented here, further work should be done to fully assess LakeFlow's performance. First, expanding the analysis to contain many more lakes spanning a variety of conditions would help to determine which factors (e.g. lake size, climate) are the dominant control on LakeFlow performance. To determine

LakeFlow's benefits beyond discharge information, studies should quantify the effect of using LakeFlow estimates of Manning's n and bathymetry as a priori information in other SWOT RSQ algorithms. Further work is also needed to better characterize the importance of including ancillary data in LakeFlow as these data, on average, improve LakeFlow discharge estimates while decreasing bathymetric accuracy. Future work should also investigate whether additional ancillary data (e.g. water withdrawal, groundwater outflows) can improve LakeFlow's ability to estimate inflows and outflows. Finally, running LakeFlow with real SWOT data will allow for a more accurate assessment of LakeFlow performance. Running LakeFlow at the global scale using SWOT observations requires a harmonized lake and river dataset to link river reaches to lakes and to identify these reaches as inflows or outflows. This dataset is currently being developed and will enable the further understanding of river-lake interactions worldwide.

Overall, this study presents a first step in bridging river and lake hydrology with satellite remote sensing, illuminating a path forward for monitoring river-lake dynamics globally. Potential applications of LakeFlow include informing reservoir operations for flood control or optimizing the distribution of freshwater resources to humans and ecosystems (Boulange et al., 2021; Grimaldi et al., 2016; Munier et al., 2015). LakeFlow could also be used to provide estimates of water residence time in lakes which could offer insights into the variability of lake greenhouse gas emissions (Maavara et al., 2020, 2019), sediment supply of rivers and lakes (Kondolf et al., 2014; Lewis et al., 2013; Wisser et al., 2013), and lotic-lentic ecosystem connectivity (Harvey and Schmadel, 2021). Applied at the global scale, LakeFlow could potentially enhance our ability to monitor and understand the impact of reservoir operations on the global water cycle.

## 5. Conclusion

The LakeFlow algorithm applies observations from SWOT to a river-lake mass conservation framework to estimate river discharge at lake inflows and outflows. We applied LakeFlow on three sample lakes spanning a variety of physiographic conditions using a synthetic dataset of SWOT-like measurements. Our findings suggest that LakeFlow can provide accurate discharge estimates of river-lake boundaries using data from the SWOT satellite. Specifically, LakeFlow captures the flow dynamics at all of the SWOT-observable inflow and outflow reaches in this study with NSE values ranging from 0.46-0.95, similar or better to other SWOT RSQ algorithm performance (Frasson et al., 2021). Incorporating lateral inflow and lake evaporation ancillary datasets into LakeFlow typically improves performance, although the impact of ancillary datasets on algorithm efficacy will be clearer once SWOT data becomes available in sufficient quantities. LakeFlow can improve upon prior estimates of bathymetry, which may prove beneficial for other SWOT RSQ algorithms, with relevance to the SWOT Confluence program. Estimating discharge at reservoir inflow and outflow reaches will improve our understanding of reservoir regulations' effect on river discharge. LakeFlow is a step toward integrating remote sensing of lake storage variability and river discharge to provide a more comprehensive view of surface water dynamics.

## 6. Acknowledgements

This work was supported by the NASA SWOT Science Team (grant #80NSSC20K1143) and the Texas Space Grant Consortium. Craig Brinkerhoff was funded by a NASA Future Investigators in Earth and Space Science Fellowship (80NSSC21K1591). The authors would like to acknowledge Aote Xin and Sarah Sorel at Kansas State University for their assistance in synthetic data generation.

## 7. Open Research

The LakeFlow outputs and synthetic SWOT data are openly available on Zenodo (https://zenodo.org/record/7781510#.ZCQ2lOjMIuU) and the code used in this analysis can be found on GitHub (https://github.com/Ryan-Riggs/Lakeflow). All data used to develop the synthetic datasets are publicly available: Landsat data (https://global-surface-water.appspot.com/download), U.S. Geological Survey gauge data (https://waterdata.usgs.gov/nwis/rt), evaporation data (https://zenodo.org/record/4646621#.ZA3qaujMIuV), and GRADES hydrological model outputs (https://www.reachhydro.org/home/records/grades).

## 8. References


Allen, G.H., Pavelsky, T.M., 2018. Global extent of rivers and streams. Science 361, 585–588. https://doi.org/10.1126/science.aat0636

Altenau, E.H., Pavelsky, T.M., Durand, M.T., Yang, X., Frasson, R.P. de M., Bendezu, L., 2021. The Surface Water and Ocean Topography (SWOT) Mission River Database (SWORD): A Global River Network for Satellite Data Products. Water Resour. Res. 57, e2021WR030054. https://doi.org/10.1029/2021WR030054

Arcement, G.J., Schneider, V.R., 1989. Guide for selecting Manning’s roughness coefficients for natural channels and flood plains (No. 2339). U.S. Geological Survey. https://doi.org/10.3133/wsp2339

Barnett, T.P., Pierce, D.W., 2008. When will Lake Mead go dry? Water Resour. Res. 44. https://doi.org/10.1029/2007WR006704

Batalla, R.J., Gómez, C.M., Kondolf, G.M., 2004. Reservoir-induced hydrological changes in the Ebro River basin (NE Spain). J. Hydrol. 290, 117–136. https://doi.org/10.1016/j.jhydrol.2003.12.002

Biancamaria, S., Lettenmaier, D.P., Pavelsky, T.M., 2016. The SWOT Mission and Its Capabilities for Land Hydrology. Surv. Geophys. 37, 307–337. https://doi.org/10.1007/s10712-015-9346-y

Bonnema, M.G., Hossain, F., 2019. Assessing the Potential of the Surface Water and Ocean Topography Mission for Reservoir Monitoring in the Mekong River Basin. Water Resour. Res. 55, 444–461. https://doi.org/10.1029/2018WR023743

Bonnema, M.G., Sikder, S., Hossain, F., Durand, M., Gleason, C.J., Bjerklie, D.M., 2016a. Benchmarking wide swath altimetry-based river discharge estimation algorithms for the Ganges river system. Water Resour. Res. 52, 2439–2461. https://doi.org/10.1002/2015WR017296

Bonnema, M.G., Sikder, S., Miao, Y., Chen, X., Hossain, F., Ara Pervin, I., Mahbubur Rahman, S.M., Lee, H., 2016b. Understanding satellite-based monthly-to-seasonal reservoir outflow estimation as a function of hydrologic controls. Water Resour. Res. 52, 4095–4115. https://doi.org/10.1002/2015WR017830

Boulange, J., Hanasaki, N., Yamazaki, D., Pokhrel, Y., 2021. Role of dams in reducing global flood exposure under climate change. Nat. Commun. 12, 417. https://doi.org/10.1038/s41467-020-20704-0

Brazil National Water Agency, 2022. National Water and Sanitation Agency (ANA) [WWW Document]. Agência Nac. Águas E Saneam. Básico ANA. URL https://www.gov.br/ana/en/national_water_agency (accessed 6.7.22).

Brinkerhoff, C.B., Gleason, C.J., Feng, D., Lin, P., 2020. Constraining Remote River Discharge Estimation Using Reach-Scale Geomorphology. Water Resour. Res. 56, e2020WR027949. https://doi.org/10.1029/2020WR027949

Brinkerhoff, C.B., Gleason, C.J., Zappa, C.J., Raymond, P.A., Harlan, M.E., 2022. Remotely Sensing River Greenhouse Gas Exchange Velocity Using the SWOT Satellite. Glob. Biogeochem. Cycles 36, e2022GB007419. https://doi.org/10.1029/2022GB007419

Busker, T., Roo, A. de, Gelati, E., Schwatke, C., Adamovic, M., Bisselink, B., Pekel, J.-F., Cottam, A., 2019. A global lake and reservoir volume analysis using a surface water dataset and satellite altimetry. Hydrol. Earth Syst. Sci. 23, 669–690. https://doi.org/10.5194/hess-23-669-2019

Chadwick, C., Gironás, J., Barría, P., Vicuña, S., Meza, F., 2021. Assessing Reservoir Performance under Climate Change. When Is It Going to Be Too Late If Current Water Management Is Not Changed? Water 13, 64. https://doi.org/10.3390/w13010064

Cohen, S., Kettner, A.J., Syvitski, J.P.M., 2014. Global suspended sediment and water discharge dynamics between 1960 and 2010: Continental trends and intra-basin sensitivity. Glob. Planet. Change 115, 44–58. https://doi.org/10.1016/j.gloplacha.2014.01.011

Cooley, S.W., Ryan, J.C., Smith, L.C., 2021. Human alteration of global surface water storage variability. Nature 591, 78–81. https://doi.org/10.1038/s41586-021-03262-3

Crétaux, J.-F., Arsen, A., Calmant, S., Kouraev, A., Vuglinski, V., Bergé-Nguyen, M., Gennero, M.-C., Nino, F., Abarca Del Rio, R., Cazenave, A., Maisongrande, P., 2011. SOLS: A lake database to monitor in the Near Real Time water level and storage variations from remote sensing data. Adv. Space Res. 47, 1497–1507. https://doi.org/10.1016/j.asr.2011.01.004

Do, H.X., Gudmundsson, L., Leonard, M., Westra, S., 2018. The Global Streamflow Indices and Metadata Archive (GSIM) – Part 1: The production of a daily streamflow archive and metadata. Earth Syst. Sci. Data 10, 765–785. https://doi.org/10.5194/essd-10-765-2018

Doll, P., Fiedler, K., Zhang, J., 2009. Global-scale analysis of river flow alterations due to water withdrawals and reservoirs. Hydrol Earth Syst Sci 20.

Durand, M., Gleason, C.J., Garambois, P.A., Bjerklie, D., Smith, L.C., Roux, H., Rodriguez, E., Bates, P.D., Pavelsky, T.M., Monnier, J., Chen, X., Baldassarre, G.D., Fiset, J.-M., Flipo, N., Frasson, R.P. d M., Fulton, J., Goutal, N., Hossain, F., Humphries, E., Minear, J.T., Mukolwe, M.M., Neal, J.C., Ricci, S., Sanders, B.F., Schumann, G., Schubert, J.E., Vilmin, L., 2016. An intercomparison of remote sensing river discharge estimation algorithms from measurements of river height, width, and slope. Water Resour. Res. 52, 4527–4549. https://doi.org/10.1002/2015WR018434

Durand, M., Gleason, C.J., Pavelsky, T.M., Frasson, R.P. de M., Turmon, M.J., David, C.H., Altenau, E.H., Tebaldi, N., Larnier, K., Monnier, J., Malaterre, P.-O., Oubanas, H., Allen, G.H., Bates, P.D., Bjerklie, D.M., Coss, S.P., Dudley, R.W., Fenoglio Marc, L., Garambois, P.-A., Lin, P., Margulis, S.A., Matte, P., Minear, J.T., Muhebwa, A., Pan, M., Peters, D., Riggs, R.M., Tarpanelli, A., Schulze, K., Tourian, M.J., Wang, J., 2023. A framework for estimating global river discharge from the Surface Water and Ocean Topography satellite mission. https://doi.org/10.1002/essoar.10508946.1

Durand, M., Neal, J., Rodríguez, E., Andreadis, K.M., Smith, L.C., Yoon, Y., 2014. Estimating reach-averaged discharge for the River Severn from measurements of river water surface elevation and slope. J. Hydrol. 511, 92–104. https://doi.org/10.1016/j.jhydrol.2013.12.050

Everard, M., Powell, A., 2002. Rivers as living systems. Aquat. Conserv. Mar. Freshw. Ecosyst. 12, 329–337. https://doi.org/10.1002/aqc.533

Feng, D., Gleason, C.J., Lin, P., Yang, X., Pan, M., Ishitsuka, Y., 2021. Recent changes to Arctic river discharge. Nat. Commun. 12, 6917. https://doi.org/10.1038/s41467-021-27228-1

Frasson, R.P. de M., Durand, M.T., Larnier, K., Gleason, C., Andreadis, K.M., Hagemann, M., Dudley, R., Bjerklie, D., Oubanas, H., Garambois, P.-A., Malaterre, P.-O., Lin, P., Pavelsky, T.M., Monnier, J., Brinkerhoff, C.B., David, C.H., 2021. Exploring the Factors Controlling the Error Characteristics of the Surface Water and Ocean Topography Mission Discharge Estimates. Water Resour. Res. 57, e2020WR028519. https://doi.org/10.1029/2020WR028519

Gao, H., 2015. Satellite remote sensing of large lakes and reservoirs: from elevation and area to storage. WIREs Water 2, 147–157. https://doi.org/10.1002/wat2.1065

Gardner, J.R., Pavelsky, T.M., Doyle, M.W., 2019. The Abundance, Size, and Spacing of Lakes and Reservoirs Connected to River Networks. Geophys. Res. Lett. 46, 2592–2601. https://doi.org/10.1029/2018GL080841

Gleason, C.J., Durand, M., 2020. Remote Sensing of River Discharge: A Review and a Framing for the Discipline. Remote Sens. 12, 1107. https://doi.org/10.3390/rs12071107

Gleason, C.J., Hamdan, A.N., 2017. Crossing the (watershed) divide: satellite data and the changing politics of international river basins. Geogr. J. 183, 2–15. https://doi.org/10.1111/geoj.12155

Grimaldi, S., Li, Y., Pauwels, V.R.N., Walker, J.P., 2016. Remote Sensing-Derived Water Extent and Level to Constrain Hydraulic Flood Forecasting Models: Opportunities and Challenges. Surv. Geophys. 37, 977–1034. https://doi.org/10.1007/s10712-016-9378-y

Gudmundsson, L., Do, H.X., Leonard, M., Westra, S., 2018. The Global Streamflow Indices and Metadata Archive (GSIM) – Part 2: Quality control, time-series indices and homogeneity assessment. Earth Syst. Sci. Data 10, 787–804. https://doi.org/10.5194/essd-10-787-2018

Hagemann, M.W., Gleason, C.J., Durand, M., 2017. BAM: Bayesian AMHG-Manning Inference of Discharge Using Remotely Sensed Stream Width, Slope, and Height. Water Resour. Res. 53, 9692–9707. https://doi.org/10.1002/2017WR021626

Harrigan, S., Zsoter, E., Alfieri, L., Prudhomme, C., Salamon, P., Wetterhall, F., Barnard, C., Cloke, H., Pappenberger, F., 2020. GloFAS-ERA5 operational global river discharge reanalysis 1979–present. Earth Syst. Sci. Data 12, 2043–2060. https://doi.org/10.5194/essd-12-2043-2020

Harvey, J.W., Schmadel, N.M., 2021. The River Corridor's Evolving Connectivity of Lotic and Lentic Waters. Front. Water 2.

Huang, L., Li, X., Fang, H., Yin, D., Si, Y., Wei, J., Liu, J., Hu, X., Zhang, L., 2019. Balancing social, economic and ecological benefits of reservoir operation during the flood season: A case study of the Three Gorges Project, China. J. Hydrol. 572, 422–434. https://doi.org/10.1016/j.jhydrol.2019.03.009

Keys, T.A., Scott, D.T., 2018. Monitoring volumetric fluctuations in tropical lakes and reservoirs using satellite remote sensing. Lake Reserv. Manag. 34, 154–166. https://doi.org/10.1080/10402381.2017.1402226

Kondolf, G.M., Gao, Y., Annandale, G.W., Morris, G.L., Jiang, E., Zhang, J., Cao, Y., Carling, P., Fu, K., Guo, Q., Hotchkiss, R., Peteuil, C., Sumi, T., Wang, H.-W., Wang, Z., Wei, Z., Wu, B., Wu, C., Yang, C.T., 2014. Sustainable sediment management in reservoirs and regulated rivers: Experiences from five continents. Earths Future 2, 256–280. https://doi.org/10.1002/2013EF000184

Lewis, S.E., Bainbridge, Z.T., Kuhnert, P.M., Sherman, B.S., Henderson, B., Dougall, C., Cooper, M., Brodie, J.E., 2013. Calculating sediment trapping efficiencies for reservoirs in tropical settings: A case study from the Burdekin Falls Dam, NE Australia. Water Resour. Res. 49, 1017–1029. https://doi.org/10.1002/wrcr.20117

Lin, P., Pan, M., Beck, H.E., Yang, Y., Yamazaki, D., Frasson, R., David, C.H., Durand, M., Pavelsky, T.M., Allen, G.H., Gleason, C.J., Wood, E.F., 2019. Global Reconstruction of Naturalized River Flows at 2.94 Million Reaches. Water Resour. Res. 55, 6499–6516. https://doi.org/10.1029/2019WR025287

Maavara, T., Chen, Q., Van Meter, K., Brown, L.E., Zhang, J., Ni, J., Zarfl, C., 2020. River dam impacts on biogeochemical cycling. Nat. Rev. Earth Environ. 1, 103–116. https://doi.org/10.1038/s43017-019-0019-0

Maavara, T., Lauerwald, R., Laruelle, G.G., Akbarzadeh, Z., Bouskill, N.J., Van Cappellen, P., Regnier, P., 2019. Nitrous oxide emissions from inland waters: Are IPCC estimates too high? Glob. Change Biol. 25, 473–488. https://doi.org/10.1111/gcb.14504

Macklin, M.G., Lewin, J., 2015. The rivers of civilization. Quat. Sci. Rev. 114, 228–244. https://doi.org/10.1016/j.quascirev.2015.02.004

Munier, S., Polebistki, A., Brown, C., Belaud, G., Lettenmaier, D.P., 2015. SWOT data assimilation for operational reservoir management on the upper Niger River Basin. Water Resour. Res. 51, 554–575. https://doi.org/10.1002/2014WR016157

Nickles, C., Beighley, E., 2021. Leveraging River Network Topology and Regionalization to Expand SWOT-Derived River Discharge Time Series in the Mississippi River Basin. Remote Sens. 13, 1590. https://doi.org/10.3390/rs13081590

Pavelsky, T.M., Durand, M.T., Andreadis, K.M., Beighley, R.E., Paiva, R.C.D., Allen, G.H., Miller, Z.F., 2014. Assessing the potential global extent of SWOT river discharge observations. J. Hydrol. 519, 1516–1525. https://doi.org/10.1016/j.jhydrol.2014.08.044

Pekel, J.-F., Cottam, A., Gorelick, N., Belward, A.S., 2016. High-resolution mapping of global surface water and its long-term changes. Nature 540, 418–422. https://doi.org/10.1038/nature20584

Ryan, J.C., Smith, L.C., Cooley, S.W., Pitcher, L.H., Pavelsky, T.M., 2020. Global Characterization of Inland Water Reservoirs Using ICESat-2 Altimetry and Climate Reanalysis. Geophys. Res. Lett. 47, e2020GL088543. https://doi.org/10.1029/2020GL088543

Sheng, Y., Song, C., Wang, J., Lyons, E.A., Knox, B.R., Cox, J.S., Gao, F., 2016. Representative lake water extent mapping at continental scales using multi-temporal Landsat-8 imagery. Remote Sens. Environ., Landsat 8 Science Results 185, 129–141. https://doi.org/10.1016/j.rse.2015.12.041

Shiklomanov, A.I., Lammers, R.B., 2009. Record Russian river discharge in 2007 and the limits of analysis. Environ. Res. Lett. 4, 045015. https://doi.org/10.1088/1748-9326/4/4/045015

Smith, L.C., 1997. Satellite remote sensing of river inundation area, stage, and discharge: a review. Hydrol. Process. 11, 1427–1439. https://doi.org/10.1002/(SICI)1099-1085(199708)11:10<1427::AID-HYP473>3.0.CO;2-S

Stan Development Team, 2023. Stan Modeling Language Users Guide and Reference Manual.

Tayfur, G., Moramarco, T., Singh, V.P., 2007. Predicting and forecasting flow discharge at sites receiving significant lateral inflow. Hydrol. Process. 21, 1848–1859. https://doi.org/10.1002/hyp.6320

Tian, W., Liu, X., Wang, K., Bai, P., Liu, C., Liang, X., 2022. Estimation of global reservoir evaporation losses. J. Hydrol. 607, 127524. https://doi.org/10.1016/j.jhydrol.2022.127524

Tuozzolo, S., Lind, G., Overstreet, B., Mangano, J., Fonstad, M., Hagemann, M., Frasson, R.P.M., Larnier, K., Garambois, P.-A., Monnier, J., Durand, M., 2019. Estimating River Discharge With Swath Altimetry: A Proof of Concept Using AirSWOT Observations. Geophys. Res. Lett. 46, 1459–1466. https://doi.org/10.1029/2018GL080771

UNEP, 2016. Transboundary River Basins Status and Trends, Summary for Policy Makers, River Basins. United Nations Environment Programme.

U.S. Geological Survey, 2022. USGS Current Water Data for the Nation [WWW Document]. US Geol. Surv. URL https://waterdata.usgs.gov/nwis/rt (accessed 5.1.21).

Vörösmarty, C.J., Green, P., Salisbury, J., Lammers, R.B., 2000. Global Water Resources: Vulnerability from Climate Change and Population Growth. Science 289, 284–288. https://doi.org/10.1126/science.289.5477.284

Wang, F., Maberly, S.C., Wang, B., Liang, X., 2018. Effects of dams on riverine biogeochemical cycling and ecology. Inland Waters 8, 130–140. https://doi.org/10.1080/20442041.2018.1469335

Wang, J., Sheng, Y., Gleason, C.J., Wada, Y., 2013. Downstream Yangtze River levels impacted by Three Gorges Dam. Environ. Res. Lett. 8, 044012. https://doi.org/10.1088/1748-9326/8/4/044012

Wang, J., Sheng, Y., Wada, Y., 2017. Little impact of the Three Gorges Dam on recent decadal lake decline across China's Yangtze Plain. Water Resour. Res. 53, 3854–3877. https://doi.org/10.1002/2016WR019817

Wisser, D., Frolking, S., Hagen, S., Bierkens, M.F.P., 2013. Beyond peak reservoir storage? A global estimate of declining water storage capacity in large reservoirs. Water Resour. Res. 49, 5732–5739. https://doi.org/10.1002/wrcr.20452

Yang, T., Zhang, Q., Chen, Y.D., Tao, X., Xu, C., Chen, X., 2008. A spatial assessment of hydrologic alteration caused by dam construction in the middle and lower Yellow River, China. Hydrol. Process. 22, 3829–3843. https://doi.org/10.1002/hyp.6993

Yang, X., Pavelsky, T.M., Ross, M.R.V., Januchowski-Hartley, S.R., Dolan, W., Altenau, E.H., Belanger, M., Byron, D., Durand, M., Van Dusen, I., Galit, H., Jorissen, M., Langhorst, T., Lawton, E., Lynch, R., Mcquillan, K.A., Pawar, S., Whittemore, A., 2022. Mapping Flow-Obstructing Structures on Global Rivers. Water Resour. Res. 58, e2021WR030386. https://doi.org/10.1029/2021WR030386

Yevjevich, V., 1992. Water and Civilization. Water Int. 17, 163–171. https://doi.org/10.1080/02508069208686135

Yoon, Y., Beighley, E., 2015. Simulating streamflow on regulated rivers using characteristic reservoir storage patterns derived from synthetic remote sensing data. Hydrol. Process. 29, 2014–2026. https://doi.org/10.1002/hyp.10342

Yoon, Y., Beighley, E., Lee, H., Pavelsky, T., Allen, G., 2016. Estimating Flood Discharges in Reservoir-Regulated River Basins by Integrating Synthetic SWOT Satellite Observations and Hydrologic Modeling. J. Hydrol. Eng. 21, 05015030. https://doi.org/10.1061/(ASCE)HE.1943-5584.0001320

Zhao, G., Gao, H., 2019. Estimating reservoir evaporation losses for the United States: Fusing remote sensing and modeling approaches. Remote Sens. Environ. 226, 109–124. https://doi.org/10.1016/j.rse.2019.03.015

Zhao, G., Li, Y., Zhou, L., Gao, H., 2022. Evaporative water loss of 1.42 million global lakes. Nat. Commun. 13, 3686. https://doi.org/10.1038/s41467-022-31125-6

# Turning lakes into river gauges using the LakeFlow algorithm

Ryan M. Riggs[1], George H. Allen[2], Craig B. Brinkerhoff[3], Md. Safat Sikder[4], Jida Wang[4]
(1)Department of Geography, Texas A&M University, College Station, TX, USA, (2)Department of Geosciences, Virginia Polytechnic Institute and State University, Blacksburg, VA, USA, (3)Department of Civil and Environmental Engineering, University of Massachusetts Amherst, Amherst, MA, USA, (4)Department of Geography and Geospatial Sciences, Kansas State University, Manhattan, KS, USA.

**Key points:**

1. LakeFlow is a new algorithm that uses SWOT satellite data to estimate river inflow and outflow at lakes via mass conservation.
2. Applying LakeFlow to three sample lake systems shows promising performance for estimating lake inflows and outflows (median NSE = 0.88).
3. Including modeled estimates of non SWOT-observed evaporation and tributary inflows can further improve LakeFlow discharge estimates.

**Abstract**

Rivers and lakes are intrinsically connected waterbodies yet they are rarely used to hydrologically constrain one another with remote sensing. Here we begin to bridge the gap between river and lake hydrology with the introduction of the LakeFlow algorithm. LakeFlow uses river-lake mass conservation and observations from the Surface Water and Ocean Topography (SWOT) satellite to provide river discharge estimates of lake and reservoir inflows and outflows. We test LakeFlow performance at three lakes using a synthetic SWOT dataset containing the maximum measurement errors defined by the mission science requirements, and we include modeled lateral inflow and lake evaporation data to further constrain the mass balance. We find that LakeFlow produces promising discharge estimates (median Nash-Sutcliffe efficiency=0.88, relative bias=14%). LakeFlow can inform water resources management by providing global lake inflow and outflow estimates, highlighting a path for recognizing rivers and lakes as an interconnected system.

**Plain language summary**

Effective water resource management depends on our ability to monitor and understand lake and reservoir inflows and outflows. Satellite remote sensing of lakes and rivers has become increasingly important for water management but little work has been done to estimate streamflow at river-lake interfaces. Here we present the LakeFlow algorithm that leverages satellite observations of lakes and rivers to estimate streamflow at lake inflows and outflows. We test LakeFlow at three U.S. lakes in Georgia, Arizona and Kansas, and find that it provides promising estimates of streamflow at river-lake boundaries. LakeFlow provides valuable insights into river-lake streamflow dynamics, which can inform water management decisions and is a step forward in the integration of river and lake studies.

## 1. Introduction

Rivers and lakes serve as vital sources of freshwater for ecosystems and civilizations worldwide (Everard and Powell, 2002; Macklin and Lewin, 2015; Yevjevich, 1992). While rivers and lakes are often treated as separate systems in large-scale remote sensing studies, their hydrologies are intimately related such that hydrologic changes in one water body type can be used to constrain the hydrology of an adjacent water body of a different type (Vörösmarty et al., 2000). For example, the relationship between inflow and outflow of a natural lake or human-made reservoir (hereinafter collectively referred to as a “lake” unless otherwise stated) can control the lake’s volumetric water storage and water surface elevation. Natural lakes located along river networks can attenuate local discharge downstream and actively managed reservoirs can significantly affect downstream flow regime by altering the natural timing and quantity of river discharge (Doll et al., 2009; Wang et al., 2017; Yang et al., 2022). Reservoir inflow and outflow dynamics are key for modeling reservoir operations, which can be difficult to simulate from water mass balance alone, especially at the continental to global scale (Cohen et al., 2014; Harrigan et al., 2020).

At these large scales, understanding of the hydrologic interplay between rivers and lakes has largely been developed through the analysis of streamflow gauges located on lake inflows and outflows (i.e., the rivers flowing into and out of a lake), as well as lake-level gauges (Batalla et al., 2004; Shiklomanov and Lammers, 2009; Yang et al., 2008). Unfortunately, most of Earth’s lakes do not have publicly available gauge data and those that do are primarily located on large lakes or in a few geographically isolated regions (Brazil National Water Agency, 2022; Do et al., 2018; Gudmundsson et al., 2018; U.S. Geological Survey, 2022). This lack of observational data limits our understanding of how impoundments impact surface water flows and has motivated the development of alternative techniques for supplementing river and lake gauge observations.

Satellite remote sensing is uniquely capable of providing observation-based discharge estimates in near-real time and at the global scale (Smith, 1997). Although remote sensing of discharge (RSQ) has been performed using a variety of satellite data and techniques (Gleason and Durand, 2020), much of the recent focus has been in preparation for the recently launched Surface Water and Ocean Topography (SWOT) mission (Biancamaria et al., 2016). Though SWOT cannot directly observe river discharge, it can potentially provide unprecedented cotemporal measurements of river area, elevation, width, and slope for all rivers within the SWOT River Database (SWORD) (Altenau et al., 2021). The SWOT mission will also produce discharge estimates calculated by combining cotemporal SWOT observations with flow laws (e.g. hydraulic geometry, Manning's equation), mass conservation principles, and a priori estimates of non-SWOT-observable flow-law parameters (FLP) such as frictional resistance (Manning's n) and bathymetry (Brinkerhoff et al., 2020; Durand et al., 2014). These SWOT discharge estimates will be practically produced using the Confluence program which houses several different RSQ algorithms (Durand et al., 2023). SWOT RSQ algorithms are sensitive to FLP estimates (Durand et al., 2016) which are provided by the SWORD of Science (SoS) database for all rivers in SWORD (Brinkerhoff et al., 2020). SoS priors of Manning's n and bathymetry are developed using *in situ* measurements that are then paired with river attributes such as mean width, allowing for mean width alone to provide prior estimates of these FLPs. Although SWOT discharge is expected to improve our understanding of global river discharge (Pavelsky et al., 2014), existing SWOT RSQ algorithms do not leverage SWOT observations of lakes into their workflow, which could improve performance.

In lakes, SWOT can observe lake surface area and elevation, which together can be combined to estimate volumetric storage change (Busker et al., 2019; Crétaux et al., 2011; Gao, 2015; Zhao and Gao, 2019). Storage change estimates are valuable for understanding seasonal and long-term trends in water availability and usage (Cooley et al., 2021; Keys and Scott, 2018; Ryan et al., 2020). Storage change fluctuations also influence downstream river discharge

(Nickles and Beighley, 2021; Wang et al., 2013) but very few remote sensing applications consider lakes and rivers as an interconnected system (Gardner et al., 2019). The few remote sensing studies that do assess lakes and rivers together rely on modeled discharge and use satellite estimates of lake storage change to revise the modeled outflow discharge (Bonnema and Hossain, 2019; Yoon et al., 2016; Yoon and Beighley, 2015). This calibration only improves the difference between the inflow and outflow discharge, leaving the original bias in the modeled inflow (or outflow) discharge uncorrected (Bonnema et al., 2016b). However, the accuracies for both inflow and outflow discharge are important because together they provide key insights into human water management and the impact lakes have on river flow regime. Currently, SWOT RSQ algorithms have neither been assessed nor are specifically designed to run at river-lake boundaries (Bonnema et al., 2016a; Durand et al., 2016; Frasson et al., 2021).

To address these gaps in our ability to monitor the river-lake continuum, we develop LakeFlow, an algorithm which applies river-lake mass conservation to estimate both lake inflow and outflow discharge. Like other SWOT RSQ algorithms, LakeFlow relies on Manning's equation and mass conservation (Feng et al., 2021; Hagemann et al., 2017) but also leverages additional SWOT observations of lake storage change to further constrain river discharge. In addition to discharge, LakeFlow estimates Manning's n and bathymetry of lake inflow and outflow channels, which can be used to inform or improve other SWOT RSQ algorithms. LakeFlow could potentially be applied to the nearly 17 thousand SWOT observable lakes that are located along the SWORD network and have at least one inflow and one outflow reach that are observable from SWOT (Figure 1). In total, LakeFlow could possibly provide valuable insights into discharge dynamics at 19,380 inflow and 16,959 outflow reaches that are connected to

SWOT observable lakes. Ultimately, LakeFlow bridges the gap between lake storage and river discharge to improve SWOT discharge coverage and accuracy.

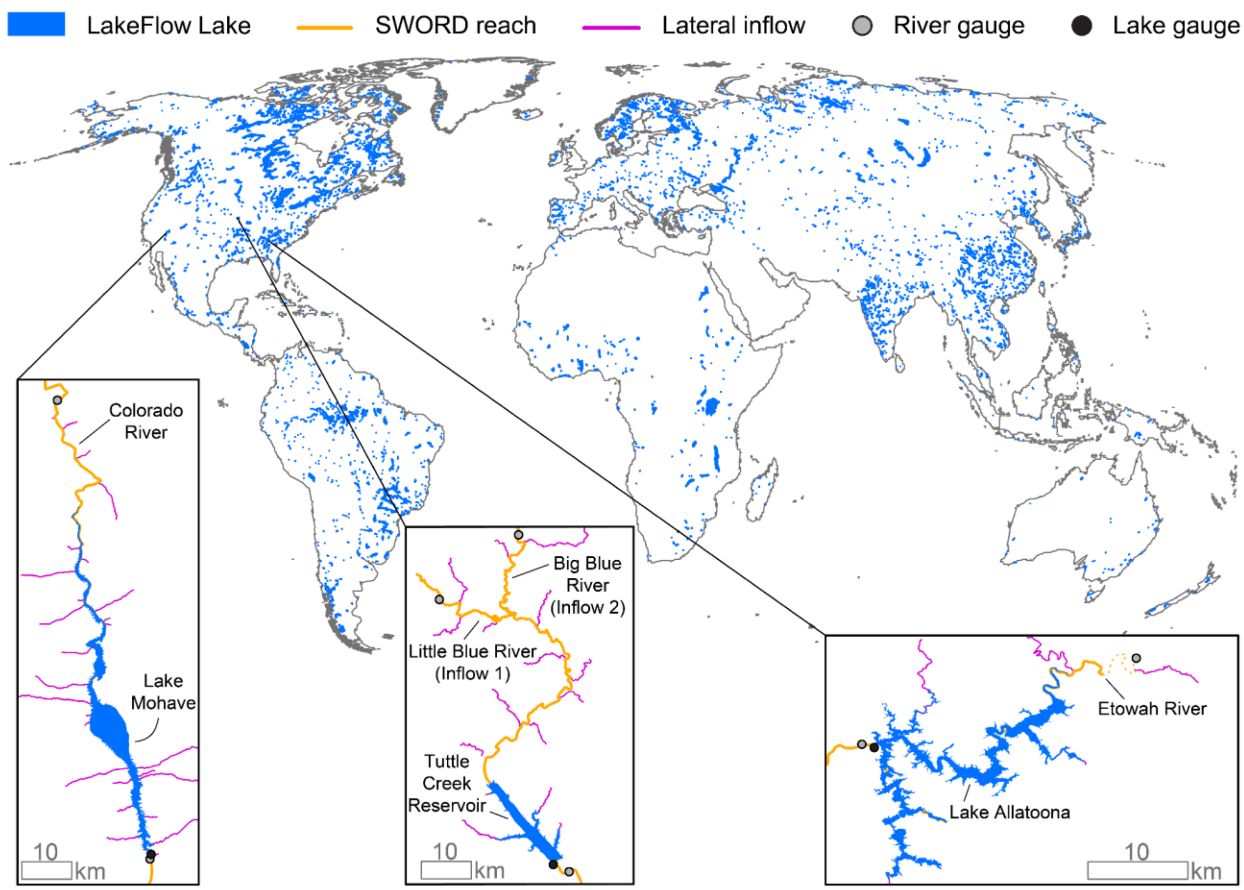


**Figure 1**. Global distribution of lakes suitable for LakeFlow implementation (N=16,610) with three sample lakes highlighted. Each of these lakes is observable by SWOT (Sheng et al., 2016) and contains at least one SWOT observable inflow and one SWOT observable outflow (Allen and Pavelsky, 2018; Altenau et al., 2021). Note the Lake Allatoona inflow gauge is located on the inflow mainstem (dashed orange line) but is located 7 km upstream of the SWORD reach (orange line).

## 2. Methods

### 2.1 LakeFlow algorithmic design

The LakeFlow algorithm uses SWOT observed river and lake variables to estimate discharge. LakeFlow uses the modified version of Manning's equation from Durand et al. (2014) to describe discharge dynamics for the inflow and outflow reaches,

$$Q = n^{-1}(A_0 + \delta A)^{5/3} W^{-2/3} S^{1/2}, \tag{1}$$

where $Q$ is discharge and $n$ is the frictional resistance of the river channel, referred to as Manning's n. $A_0$ represents the unobservable cross-sectional area that extends beyond the minimum observed water level, hereinafter referred to as bathymetry, $\delta A$ is the SWOT observable change in cross-sectional area, $W$ is river width, and $S$ is slope. LakeFlow leverages SWOT estimated lake storage change ($\delta V$) during the time period between two consecutive SWOT overpasses ($p$) to constrain inflow and outflow discharge based on mass conservation,

$$\delta V_p = \int_{t=0}^{p} \left( {n_i}^{-1}(A_{0i} + \delta A_i)^{5/3} {W_i}^{-2/3} {S_i}^{1/2} - {n_o}^{-1}(A_{0o} + \delta A_o)^{5/3} W_o^{-2/3} {S_o}^{1/2} + Q_l - E \right)_t . \tag{2}$$

Here $t$ represents any time during period $p$, $Q_l$ is lateral inflows from channels too small to been observed by SWOT, $E$ is lake evaporation, and all other variables are the same as eq. 1 with $i$ and $o$ denoting the variables of the SWOT observable inflow and outflow reaches, respectively (Figure 2). Simply put, LakeFlow assumes that lake storage change is equal to inflow minus outflow discharge while accounting for lateral inflows and evaporation. While SWOT provides estimates of lake storage change ($\delta V$), change in river cross-sectional area ($\delta A$), slope ($S$), and width ($W$), it does not observe Manning's n ($n$) or bathymetry ($A_0$) for the inflow and outflow reaches, leaving four unknown variables in eq. 2. Note that for simplicity, we only include one inflow reach and one outflow reach for eq. 2 but LakeFlow has the capability to be applied on lakes with multiple inflow and outflow reaches.

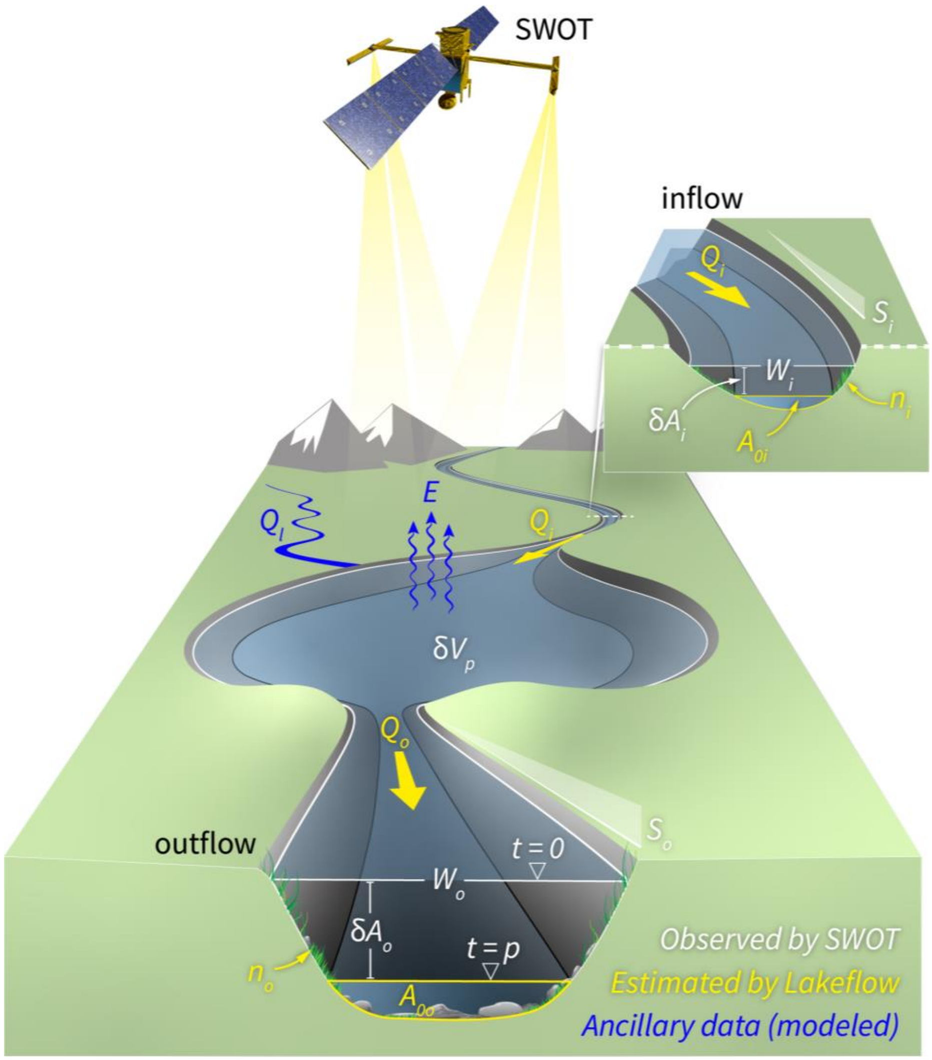


**Figure 2**. Conceptual diagram of the LakeFlow algorithm which uses repeat SWOT observations of lakes and rivers to estimate the inflows and outflows of lakes in cubic meters per second. See eq. 1 and 2 for variable definitions. Shown are two snapshots of a lake system corresponding to two SWOT overpasses (*t=0* and *t=p*). Note that time *p* corresponds to the minimum observed flow and that only SWOT observable variables are shown for *t=0*.

Like many other SWOT RSQ algorithms, LakeFlow struggles from parameter equifinality; there are roughly equal numbers of known and unknown parameters in eq. 2. Following the approach of Hagemann et al. (2017) and Brinkerhoff et al. (2022), we use

Bayesian inference to constrain the uncertainty in LakeFlow's unknown parameters ($n_i$, $A_{0i}$ , $n_o$, $A_{0o}$) given repeated SWOT observations. Bayesian approaches start from Bayes rule,

$$p(\Theta|x) = \frac{f(x|\Theta)p(\Theta)}{p(x)}, \tag{3}$$

where $\Theta$ is a set of unobserved SWOT parameters, $x$ is the SWOT observed data, $f(x|\Theta)$ is the sampling model where data are conditional on the parameters, and $p(\Theta)$is the joint prior distribution of the parameters. Thus, we are interested in approximating $p(\Theta|x)$, the posterior distribution. Bayesian inference aims to approximate the posterior distribution by assuming proportionality ( $p(\Theta|x) \propto f(x|\Theta)p(\Theta)$) and using Monte Carlo sampling. To implement the Bayesian inference, we log transform and scale Manning's equation to have integer coefficients,

$$6 \log Q = -6 \log n + 10 \log(A_0 + \delta A) - 4 \log W + 3 \log S. \tag{4}$$

To provide a likelihood equation, we rearrange eq. 4 to isolate the measured variables for both the inflow and outflow reaches,

$$4 \log W - 3 \log S = -6 \log n - 6 \log Q + 10 \log(A_0 + \delta A), \tag{5}$$

and the likelihood equation for river-lake mass conservation is,

$$\delta V - Q_l + E = exp(logQ_i) - exp(logQ_o). \tag{6}$$

The Bayesian approach requires prior estimates of all unknown parameters in eq. 2 which are taken from the SWOT SoS. In addition to estimates of Manning's n and bathymetry, the SoS provides gauge-constrained and unconstrained modeled estimates of mean flow and LakeFlow uses the gauge-constrained estimate, taken from the Global Reach-Level A Priori Discharge Estimates for SWOT (GRADES) model product (Lin et al., 2019). The Bayesian inference uses the Stan probabilistic programming language (Stan Development Team, 2023) to approximate the posterior distribution and provide estimates of all unknowns in eq. 2.

### 2.2 Datasets

We investigate the performance of LakeFlow in three sample lakes spanning a range of climate regions as seen in Figure 1: Lake Allatoona (humid); Lake Mohave (arid); and Tuttle Creek Reservoir (semi-arid). Lake Allatoona (area: 36 $km^2$) is a flood control reservoir along the Etowah River in northwestern Georgia. Lake Mohave (area: 99 $km^2$) is a hydropower reservoir on the Colorado River spanning the border of Arizona and Nevada. Tuttle Creek Reservoir (area: 43 $km^2$) is located in northeastern Kansas and is built to control floods on the Little Blue and Big Blue Rivers. These lakes each have a U.S. Geological Survey (USGS) gauge station on or near their SWOT observable inflow and outflow reaches as well as on the lakes themselves. Lake Allatoona and Lake Mohave each contain one inflow and one outflow reach and Tuttle Creek Reservoir has two inflow reaches.

Because SWOT data are not yet available, we generate a synthetic dataset of SWOT observable variables by utilizing gauge records from the USGS (U.S. Geological Survey, 2022), a Landsat-based water occurrence map (Pekel et al., 2016), and a priori channel attributes provided in SWORD. We then corrupt these data to produce SWOT-like observations by using the measurement errors defined by the mission science requirements and limit the number of observations to one observation per week corresponding to the approximate average overpass rate of SWOT over these lakes (Biancamaria et al., 2016). The synthetic dataset is developed using hydraulic principles and contains values of non SWOT observed Manning's n and bathymetry (see Supplemental Text S1 for details of the synthetic dataset). The historical time period of the synthetic dataset is determined by the availability of USGS gauge records, such that the measurements of the lake and its inflow and outflow must all overlap in time. As a result, the timespan ($p$ in eq. 2) for each of the three lakes is 10/01/2009 to 09/30/2014 for Lake Allatoona, 10/01/2008 to 09/30/2013 for Lake Mohave, and 10/01/2006 to 09/30/2011 for Tuttle Creek Reservoir.

Where the LakeFlow algorithm can run, lake storage change is predominantly governed by large-river inflows and outflows that are observable by SWOT, but lake storage change can also be influenced by other factors including inflow from groundwater runoff, small lateral streams (pink lines in Figure 1), and evaporation loss (Tayfur et al., 2007; Tian et al., 2022; Zhao et al., 2022). To study the impact of including these factors on LakeFlow's performance, we run two scenarios of LakeFlow: one that only includes SWOT-based observations and a second that includes SWOT observations and also ancillary datasets of lateral inflow and evaporation, represented by $Q_l$ and $E$ in eq. 2, respectively. We estimate lateral inflow using high-resolution simulated discharge from GRADES (Lin et al., 2019) and we estimate evaporation losses using modeled data from the Global Lake Evaporation Volume (GLEV) dataset (Zhao et al., 2022) (see Supplemental Text S2 for details of these ancillary datasets). We then assess LakeFlow's performance related to the ancillary datasets for each of the three study sites by comparing same-day LakeFlow estimated discharge with gauge discharge from the USGS and calculate Nash-Sutcliffe Efficiency (NSE), relative bias (rBias), normalized root-mean-square error (NRMSE), and mean absolute error (MAE) (Table S1). In addition to assessing discharge accuracy, we compare LakeFlow FLP estimates with the synthetic dataset's values of Manning's n and bathymetry. We further compare LakeFlow FLP estimates with the SoS prior estimates to assess LakeFlow's capabilities for informing other SWOT-based RSQ algorithms. The SoS FLPs are chosen for comparison as these are the default prior FLP estimates for SWOT RSQ algorithms (Durand et al., 2023) (see section 1 for more information).

## 3. Results

The results of the analysis, generated from synthetic SWOT data at the three test sites, indicate that the LakeFlow algorithm will be able to successfully estimate lake inflows and outflows from SWOT observations. In general, we find that LakeFlow estimated discharge skillfully resembles the gauge hydrograph for all of the inflow and outflow reaches (Figure 3). However, there is clear bias on some reaches, namely the Allatoona Lake Inflow and Tuttle Creek Reservoir Inflow 1. Even where there are biases present, LakeFlow captures flow variability for each of the reaches analyzed here as evidenced by a positive NSE for all reaches and a median NSE and NRMSE of 0.88 and 29.0%, respectively. While two reaches have relatively large rBias values, all of the other reaches have an absolute rBias less than 15% with a median rBias of 13.5%, indicating that on average, LakeFlow provides near-zero discharge estimates at river-lake interfaces.

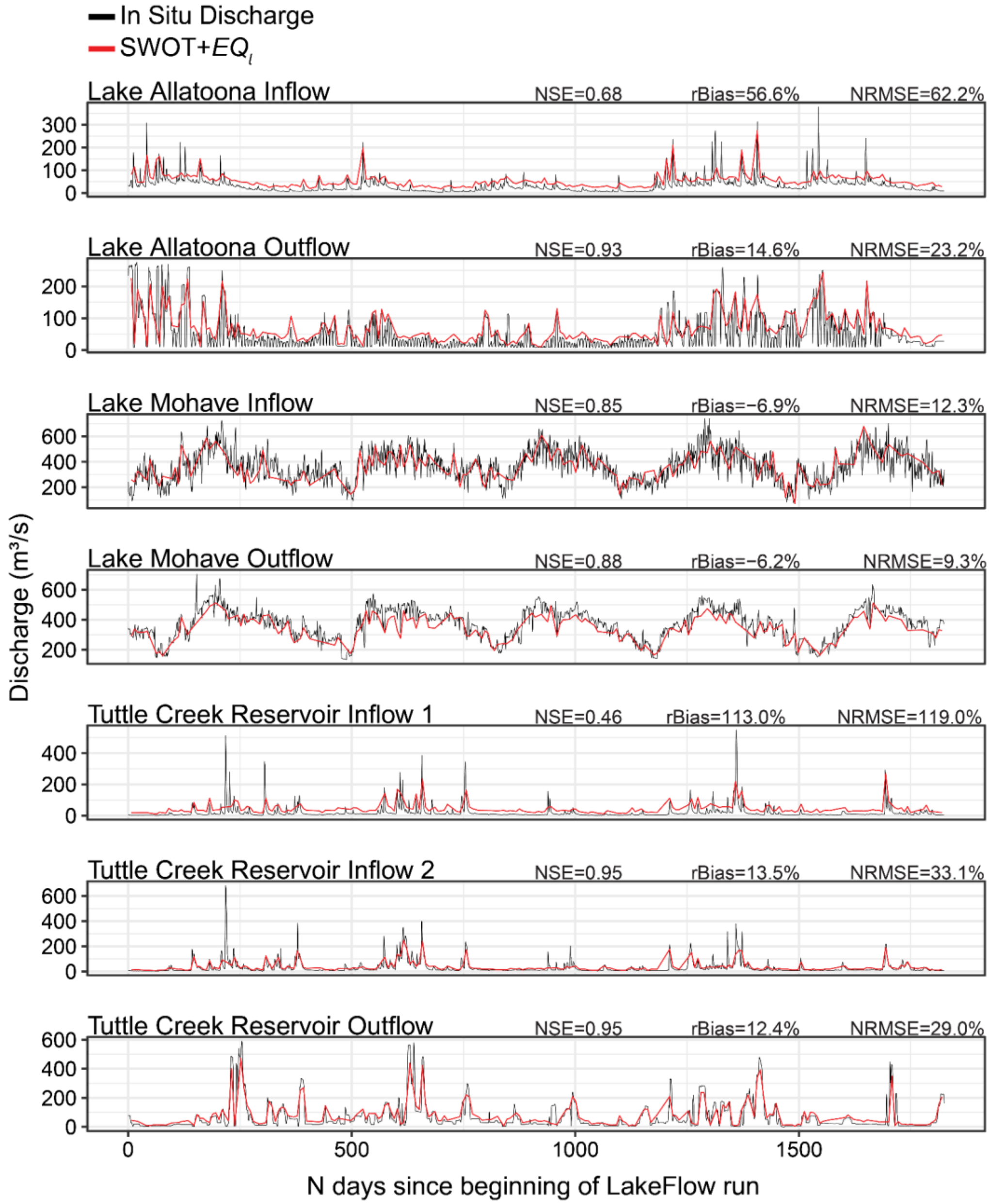


**Figure 3.** LakeFlow estimated discharge for all lake inflows and outflows compared to gauge records.

LakeFlow accurately estimates discharge dynamics across all seven study reaches (Figure 4a). Overall, LakeFlow discharge performance tends to modestly improve with the addition of the lateral inflow and evaporation ancillary datasets but does not tend to improve with the addition of only a single one of these datasets (Figure S1). This discrepancy is likely due to the inherent bias introduced when only including one of these ancillary terms. LakeFlow discharge mean absolute error (MAE) improves by 1.6% when both ancillary datasets are included compared to including neither. However, the bias marginally increases when both ancillary data are used but remains near-zero (Figure 4a). With and without the ancillary data, LakeFlow discharge for each study location correlates well with same-day gauge discharge observations with marginal overestimations and underestimations in low and high flows, respectively (Pearson correlation coefficient, $R$ ranges from 0.95 to 0.99).

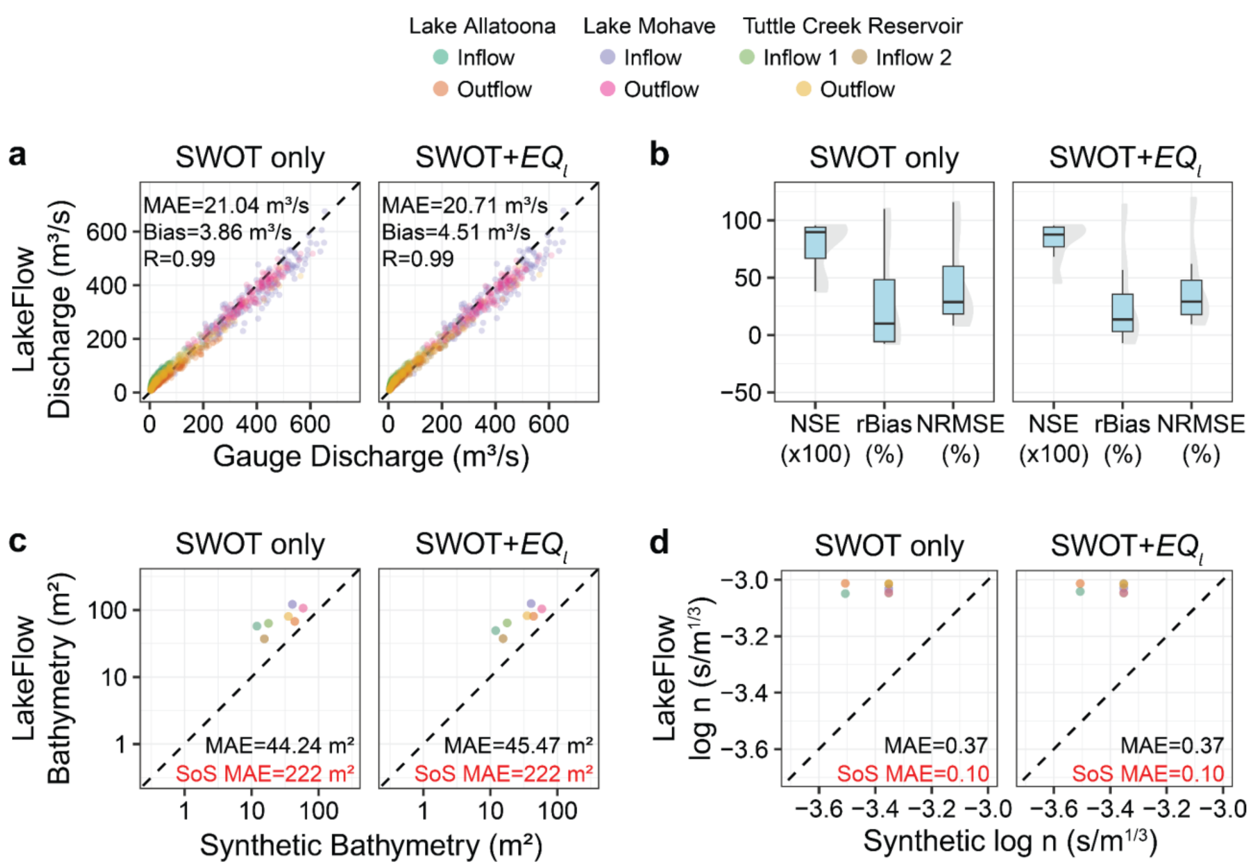


**Figure 4.** LakeFlow performance without ("SWOT only") and with ("SWOT+$EQ_l$") ancillary data. (a) Scatterplots of same-day gauge discharge vs. LakeFlow estimated discharge across all reaches. (b) Boxplots and half violin plots of LakeFlow discharge performance metrics across all

reaches: NSE (scaled by 100), rBias (%), and NRMSE (%). (c) Scatterplots of synthetic bathymetry vs. LakeFlow estimated bathymetry across all reaches. (d) Scatterplots of log synthetic Manning's n vs. log LakeFlow estimated Manning's n across all reaches.

Across all reaches, we find that discharge performance modestly improves with the addition of the ancillary data (Figure 4b). For example, the mean NSE and NRMSE improve by 4.8% and 6.7%, respectively, when including ancillary data. Conversely, there is a positive bias present in most reaches and the mean rBias is unaffected by the inclusion of the ancillary data. Nearly all of the metrics have a negatively skewed distribution, indicating that LakeFlow performs well on average but occasionally exhibits poor performance. In addition to estimating discharge, LakeFlow can estimate unobserved bathymetry ($A_0$) and Manning's n, with MAE values of 44 $m^2$ and 0.37 $s/m^{1/3}$ (log), respectively. Across all reaches and scenarios, LakeFlow MAE for bathymetry is on average 80% lower than the SoS MAE (Figure 4c) while LakeFlow estimated Manning's n values are marginally worse than the SoS (Figure 4d). LakeFlow tends to overestimate Manning's n values in the three test lakes, which may be related to bathymetry estimates having a positive bias. Bathymetric accuracy declines by 2.8% and Manning's n accuracy remains stable with the inclusion of the ancillary data.

## 4. Discussion

The LakeFlow algorithm can provide useful discharge estimates at river-lake interfaces and will enhance the SWOT mission's capabilities for monitoring surface water dynamics. We do not test LakeFlow in locations where other SWOT RSQ algorithms have been assessed, but our findings indicate that LakeFlow's discharge accuracy is comparable or better than other SWOT RSQ algorithms (Frasson et al., 2021), thus providing the capability to extend the SWOT discharge product to river-lake boundaries with no expected decline in accuracy. These discharge data can inform hydroelectric and water management decisions and improve our understanding of how reservoir dynamics affect the surrounding environment (Barnett and Pierce, 2008; Chadwick et al., 2021; Huang et al., 2019; Wang et al., 2018). Reservoir operations are particularly important in transboundary water basins where water management in upstream portions of the basin can lead to actual or perceived inequities in downstream water distribution (UNEP, 2016). However, LakeFlow inflow and outflow discharge estimates can potentially increase the transparency of reservoir management practices with implications for water management decisions within transboundary basins (Gleason and Hamdan, 2017).

In addition to discharge, LakeFlow's ability to accurately estimate Manning's n and bathymetry values could provide useful geomorphic insights near river-lake interfaces. Compared to the SoS, LakeFlow provides marginally worse Manning's n estimates but significantly more accurate bathymetric estimates. However, Manning's n values are inherently limited to a small range of 0.02-0.07 $s/m^{1/3}$ (Arcement and Schneider, 1989) whereas bathymetry varies widely globally. Since RSQ algorithms are sensitive to prior FLP estimates (Bonnema et al., 2016a; Durand et al., 2016; Tuozzolo et al., 2019), the more accurate LakeFlow bathymetries could improve the performance and efficiency of other RSQ algorithms near river-lake interfaces. Thus, there is potential to implement LakeFlow into the SWOT Confluence program (Durand et al., 2023) to inform other SWOT RSQ algorithms.

While LakeFlow is shown to perform well at the three study sites presented here, further work should be done to fully assess LakeFlow's performance. First, expanding the analysis to contain many more lakes spanning a variety of conditions would help to determine which factors (e.g. lake size, climate) are the dominant control on LakeFlow performance. To determine

LakeFlow's benefits beyond discharge information, studies should quantify the effect of using LakeFlow estimates of Manning's n and bathymetry as a priori information in other SWOT RSQ algorithms. Further work is also needed to better characterize the importance of including ancillary data in LakeFlow as these data, on average, improve LakeFlow discharge estimates while decreasing bathymetric accuracy. Future work should also investigate whether additional ancillary data (e.g. water withdrawal, groundwater outflows) can improve LakeFlow's ability to estimate inflows and outflows. Finally, running LakeFlow with real SWOT data will allow for a more accurate assessment of LakeFlow performance. Running LakeFlow at the global scale using SWOT observations requires a harmonized lake and river dataset to link river reaches to lakes and to identify these reaches as inflows or outflows. This dataset is currently being developed and will enable the further understanding of river-lake interactions worldwide.

Overall, this study presents a first step in bridging river and lake hydrology with satellite remote sensing, illuminating a path forward for monitoring river-lake dynamics globally. Potential applications of LakeFlow include informing reservoir operations for flood control or optimizing the distribution of freshwater resources to humans and ecosystems (Boulange et al., 2021; Grimaldi et al., 2016; Munier et al., 2015). LakeFlow could also be used to provide estimates of water residence time in lakes which could offer insights into the variability of lake greenhouse gas emissions (Maavara et al., 2020, 2019), sediment supply of rivers and lakes (Kondolf et al., 2014; Lewis et al., 2013; Wisser et al., 2013), and lotic-lentic ecosystem connectivity (Harvey and Schmadel, 2021). Applied at the global scale, LakeFlow could potentially enhance our ability to monitor and understand the impact of reservoir operations on the global water cycle.

## 5. Conclusion

The LakeFlow algorithm applies observations from SWOT to a river-lake mass conservation framework to estimate river discharge at lake inflows and outflows. We applied LakeFlow on three sample lakes spanning a variety of physiographic conditions using a synthetic dataset of SWOT-like measurements. Our findings suggest that LakeFlow can provide accurate discharge estimates of river-lake boundaries using data from the SWOT satellite. Specifically, LakeFlow captures the flow dynamics at all of the SWOT-observable inflow and outflow reaches in this study with NSE values ranging from 0.46-0.95, similar or better to other SWOT RSQ algorithm performance (Frasson et al., 2021). Incorporating lateral inflow and lake evaporation ancillary datasets into LakeFlow typically improves performance, although the impact of ancillary datasets on algorithm efficacy will be clearer once SWOT data becomes available in sufficient quantities. LakeFlow can improve upon prior estimates of bathymetry, which may prove beneficial for other SWOT RSQ algorithms, with relevance to the SWOT Confluence program. Estimating discharge at reservoir inflow and outflow reaches will improve our understanding of reservoir regulations' effect on river discharge. LakeFlow is a step toward integrating remote sensing of lake storage variability and river discharge to provide a more comprehensive view of surface water dynamics.

## 6. Acknowledgements

This work was supported by the NASA SWOT Science Team (grant #80NSSC20K1143) and the Texas Space Grant Consortium. Craig Brinkerhoff was funded by a NASA Future Investigators in Earth and Space Science Fellowship (80NSSC21K1591). The authors would like to acknowledge Aote Xin and Sarah Sorel at Kansas State University for their assistance in synthetic data generation.

## 7. Open Research

The LakeFlow outputs and synthetic SWOT data are openly available on Zenodo (https://zenodo.org/record/7781510#.ZCQ2lOjMIuU) and the code used in this analysis can be found on GitHub (https://github.com/Ryan-Riggs/Lakeflow). All data used to develop the synthetic datasets are publicly available: Landsat data (https://global-surface-water.appspot.com/download), U.S. Geological Survey gauge data (https://waterdata.usgs.gov/nwis/rt), evaporation data (https://zenodo.org/record/4646621#.ZA3qaujMIuV), and GRADES hydrological model outputs (https://www.reachhydro.org/home/records/grades).

## 8. References

Allen, G.H., Pavelsky, T.M., 2018. Global extent of rivers and streams. Science 361, 585–588. https://doi.org/10.1126/science.aat0636

Altenau, E.H., Pavelsky, T.M., Durand, M.T., Yang, X., Frasson, R.P. de M., Bendezu, L., 2021. The Surface Water and Ocean Topography (SWOT) Mission River Database (SWORD): A Global River Network for Satellite Data Products. Water Resour. Res. 57, e2021WR030054. https://doi.org/10.1029/2021WR030054

Arcement, G.J., Schneider, V.R., 1989. Guide for selecting Manning's roughness coefficients for natural channels and flood plains (No. 2339). U.S. Geological Survey. https://doi.org/10.3133/wsp2339

Barnett, T.P., Pierce, D.W., 2008. When will Lake Mead go dry? Water Resour. Res. 44. https://doi.org/10.1029/2007WR006704

Batalla, R.J., Gómez, C.M., Kondolf, G.M., 2004. Reservoir-induced hydrological changes in the Ebro River basin (NE Spain). J. Hydrol. 290, 117–136. https://doi.org/10.1016/j.jhydrol.2003.12.002

Biancamaria, S., Lettenmaier, D.P., Pavelsky, T.M., 2016. The SWOT Mission and Its Capabilities for Land Hydrology. Surv. Geophys. 37, 307–337. https://doi.org/10.1007/s10712-015-9346-y

Bonnema, M.G., Hossain, F., 2019. Assessing the Potential of the Surface Water and Ocean Topography Mission for Reservoir Monitoring in the Mekong River Basin. Water Resour. Res. 55, 444–461. https://doi.org/10.1029/2018WR023743

Bonnema, M.G., Sikder, S., Hossain, F., Durand, M., Gleason, C.J., Bjerklie, D.M., 2016a. Benchmarking wide swath altimetry-based river discharge estimation algorithms for the Ganges river system. Water Resour. Res. 52, 2439–2461. https://doi.org/10.1002/2015WR017296

Bonnema, M.G., Sikder, S., Miao, Y., Chen, X., Hossain, F., Ara Pervin, I., Mahbubur Rahman, S.M., Lee, H., 2016b. Understanding satellite-based monthly-to-seasonal reservoir outflow estimation as a function of hydrologic controls. Water Resour. Res. 52, 4095–4115. https://doi.org/10.1002/2015WR017830

Boulange, J., Hanasaki, N., Yamazaki, D., Pokhrel, Y., 2021. Role of dams in reducing global flood exposure under climate change. Nat. Commun. 12, 417. https://doi.org/10.1038/s41467-020-20704-0

Brazil National Water Agency, 2022. National Water and Sanitation Agency (ANA) [WWW Document]. Agência Nac. Águas E Saneam. Básico ANA. URL https://www.gov.br/ana/en/national_water_agency (accessed 6.7.22).

Brinkerhoff, C.B., Gleason, C.J., Feng, D., Lin, P., 2020. Constraining Remote River Discharge Estimation Using Reach-Scale Geomorphology. Water Resour. Res. 56, e2020WR027949. https://doi.org/10.1029/2020WR027949

Brinkerhoff, C.B., Gleason, C.J., Zappa, C.J., Raymond, P.A., Harlan, M.E., 2022. Remotely Sensing River Greenhouse Gas Exchange Velocity Using the SWOT Satellite. Glob. Biogeochem. Cycles 36, e2022GB007419. https://doi.org/10.1029/2022GB007419

Busker, T., Roo, A. de, Gelati, E., Schwatke, C., Adamovic, M., Bisselink, B., Pekel, J.-F., Cottam, A., 2019. A global lake and reservoir volume analysis using a surface water dataset and satellite altimetry. Hydrol. Earth Syst. Sci. 23, 669–690. https://doi.org/10.5194/hess-23-669-2019

Chadwick, C., Gironás, J., Barría, P., Vicuña, S., Meza, F., 2021. Assessing Reservoir Performance under Climate Change. When Is It Going to Be Too Late If Current Water Management Is Not Changed? Water 13, 64. https://doi.org/10.3390/w13010064

Cohen, S., Kettner, A.J., Syvitski, J.P.M., 2014. Global suspended sediment and water discharge dynamics between 1960 and 2010: Continental trends and intra-basin sensitivity. Glob. Planet. Change 115, 44–58. https://doi.org/10.1016/j.gloplacha.2014.01.011

Cooley, S.W., Ryan, J.C., Smith, L.C., 2021. Human alteration of global surface water storage variability. Nature 591, 78–81. https://doi.org/10.1038/s41586-021-03262-3

Crétaux, J.-F., Arsen, A., Calmant, S., Kouraev, A., Vuglinski, V., Bergé-Nguyen, M., Gennero, M.-C., Nino, F., Abarca Del Rio, R., Cazenave, A., Maisongrande, P., 2011. SOLS: A lake database to monitor in the Near Real Time water level and storage variations from remote sensing data. Adv. Space Res. 47, 1497–1507. https://doi.org/10.1016/j.asr.2011.01.004

Do, H.X., Gudmundsson, L., Leonard, M., Westra, S., 2018. The Global Streamflow Indices and Metadata Archive (GSIM) – Part 1: The production of a daily streamflow archive and metadata. Earth Syst. Sci. Data 10, 765–785. https://doi.org/10.5194/essd-10-765-2018

Doll, P., Fiedler, K., Zhang, J., 2009. Global-scale analysis of river flow alterations due to water withdrawals and reservoirs. Hydrol Earth Syst Sci 20.

Durand, M., Gleason, C.J., Garambois, P.A., Bjerklie, D., Smith, L.C., Roux, H., Rodriguez, E., Bates, P.D., Pavelsky, T.M., Monnier, J., Chen, X., Baldassarre, G.D., Fiset, J.-M., Flipo, N., Frasson, R.P. d M., Fulton, J., Goutal, N., Hossain, F., Humphries, E., Minear, J.T., Mukolwe, M.M., Neal, J.C., Ricci, S., Sanders, B.F., Schumann, G., Schubert, J.E., Vilmin, L., 2016. An intercomparison of remote sensing river discharge estimation algorithms from measurements of river height, width, and slope. Water Resour. Res. 52, 4527–4549. https://doi.org/10.1002/2015WR018434

Durand, M., Gleason, C.J., Pavelsky, T.M., Frasson, R.P. de M., Turmon, M.J., David, C.H., Altenau, E.H., Tebaldi, N., Larnier, K., Monnier, J., Malaterre, P.-O., Oubanas, H., Allen, G.H., Bates, P.D., Bjerklie, D.M., Coss, S.P., Dudley, R.W., Fenoglio Marc, L., Garambois, P.-A., Lin, P., Margulis, S.A., Matte, P., Minear, J.T., Muhebwa, A., Pan, M., Peters, D., Riggs, R.M., Tarpanelli, A., Schulze, K., Tourian, M.J., Wang, J., 2023. A framework for estimating global river discharge from the Surface Water and Ocean Topography satellite mission. https://doi.org/10.1002/essoar.10508946.1

Durand, M., Neal, J., Rodríguez, E., Andreadis, K.M., Smith, L.C., Yoon, Y., 2014. Estimating reach-averaged discharge for the River Severn from measurements of river water surface elevation and slope. J. Hydrol. 511, 92–104. https://doi.org/10.1016/j.jhydrol.2013.12.050

Everard, M., Powell, A., 2002. Rivers as living systems. Aquat. Conserv. Mar. Freshw. Ecosyst. 12, 329–337. https://doi.org/10.1002/aqc.533

Feng, D., Gleason, C.J., Lin, P., Yang, X., Pan, M., Ishitsuka, Y., 2021. Recent changes to Arctic river discharge. Nat. Commun. 12, 6917. https://doi.org/10.1038/s41467-021-27228-1

Frasson, R.P. de M., Durand, M.T., Larnier, K., Gleason, C., Andreadis, K.M., Hagemann, M., Dudley, R., Bjerklie, D., Oubanas, H., Garambois, P.-A., Malaterre, P.-O., Lin, P., Pavelsky, T.M., Monnier, J., Brinkerhoff, C.B., David, C.H., 2021. Exploring the Factors Controlling the Error Characteristics of the Surface Water and Ocean Topography Mission Discharge Estimates. Water Resour. Res. 57, e2020WR028519. https://doi.org/10.1029/2020WR028519

Gao, H., 2015. Satellite remote sensing of large lakes and reservoirs: from elevation and area to storage. WIREs Water 2, 147–157. https://doi.org/10.1002/wat2.1065
Gardner, J.R., Pavelsky, T.M., Doyle, M.W., 2019. The Abundance, Size, and Spacing of Lakes and Reservoirs Connected to River Networks. Geophys. Res. Lett. 46, 2592–2601. https://doi.org/10.1029/2018GL080841
Gleason, C.J., Durand, M., 2020. Remote Sensing of River Discharge: A Review and a Framing for the Discipline. Remote Sens. 12, 1107. https://doi.org/10.3390/rs12071107
Gleason, C.J., Hamdan, A.N., 2017. Crossing the (watershed) divide: satellite data and the changing politics of international river basins. Geogr. J. 183, 2–15. https://doi.org/10.1111/geoj.12155
Grimaldi, S., Li, Y., Pauwels, V.R.N., Walker, J.P., 2016. Remote Sensing-Derived Water Extent and Level to Constrain Hydraulic Flood Forecasting Models: Opportunities and Challenges. Surv. Geophys. 37, 977–1034. https://doi.org/10.1007/s10712-016-9378-y
Gudmundsson, L., Do, H.X., Leonard, M., Westra, S., 2018. The Global Streamflow Indices and Metadata Archive (GSIM) – Part 2: Quality control, time-series indices and homogeneity assessment. Earth Syst. Sci. Data 10, 787–804. https://doi.org/10.5194/essd-10-787-2018
Hagemann, M.W., Gleason, C.J., Durand, M., 2017. BAM: Bayesian AMHG-Manning Inference of Discharge Using Remotely Sensed Stream Width, Slope, and Height. Water Resour. Res. 53, 9692–9707. https://doi.org/10.1002/2017WR021626
Harrigan, S., Zsoter, E., Alfieri, L., Prudhomme, C., Salamon, P., Wetterhall, F., Barnard, C., Cloke, H., Pappenberger, F., 2020. GloFAS-ERA5 operational global river discharge reanalysis 1979–present. Earth Syst. Sci. Data 12, 2043–2060. https://doi.org/10.5194/essd-12-2043-2020
Harvey, J.W., Schmadel, N.M., 2021. The River Corridor's Evolving Connectivity of Lotic and Lentic Waters. Front. Water 2.
Huang, L., Li, X., Fang, H., Yin, D., Si, Y., Wei, J., Liu, J., Hu, X., Zhang, L., 2019. Balancing social, economic and ecological benefits of reservoir operation during the flood season: A case study of the Three Gorges Project, China. J. Hydrol. 572, 422–434. https://doi.org/10.1016/j.jhydrol.2019.03.009
Keys, T.A., Scott, D.T., 2018. Monitoring volumetric fluctuations in tropical lakes and reservoirs using satellite remote sensing. Lake Reserv. Manag. 34, 154–166. https://doi.org/10.1080/10402381.2017.1402226
Kondolf, G.M., Gao, Y., Annandale, G.W., Morris, G.L., Jiang, E., Zhang, J., Cao, Y., Carling, P., Fu, K., Guo, Q., Hotchkiss, R., Peteuil, C., Sumi, T., Wang, H.-W., Wang, Z., Wei, Z., Wu, B., Wu, C., Yang, C.T., 2014. Sustainable sediment management in reservoirs and regulated rivers: Experiences from five continents. Earths Future 2, 256–280. https://doi.org/10.1002/2013EF000184
Lewis, S.E., Bainbridge, Z.T., Kuhnert, P.M., Sherman, B.S., Henderson, B., Dougall, C., Cooper, M., Brodie, J.E., 2013. Calculating sediment trapping efficiencies for reservoirs in tropical settings: A case study from the Burdekin Falls Dam, NE Australia. Water Resour. Res. 49, 1017–1029. https://doi.org/10.1002/wrcr.20117
Lin, P., Pan, M., Beck, H.E., Yang, Y., Yamazaki, D., Frasson, R., David, C.H., Durand, M., Pavelsky, T.M., Allen, G.H., Gleason, C.J., Wood, E.F., 2019. Global Reconstruction of Naturalized River Flows at 2.94 Million Reaches. Water Resour. Res. 55, 6499–6516. https://doi.org/10.1029/2019WR025287
Maavara, T., Chen, Q., Van Meter, K., Brown, L.E., Zhang, J., Ni, J., Zarfl, C., 2020. River dam

impacts on biogeochemical cycling. Nat. Rev. Earth Environ. 1, 103–116. https://doi.org/10.1038/s43017-019-0019-0

Maavara, T., Lauerwald, R., Laruelle, G.G., Akbarzadeh, Z., Bouskill, N.J., Van Cappellen, P., Regnier, P., 2019. Nitrous oxide emissions from inland waters: Are IPCC estimates too high? Glob. Change Biol. 25, 473–488. https://doi.org/10.1111/gcb.14504

Macklin, M.G., Lewin, J., 2015. The rivers of civilization. Quat. Sci. Rev. 114, 228–244. https://doi.org/10.1016/j.quascirev.2015.02.004

Munier, S., Polebistki, A., Brown, C., Belaud, G., Lettenmaier, D.P., 2015. SWOT data assimilation for operational reservoir management on the upper Niger River Basin. Water Resour. Res. 51, 554–575. https://doi.org/10.1002/2014WR016157

Nickles, C., Beighley, E., 2021. Leveraging River Network Topology and Regionalization to Expand SWOT-Derived River Discharge Time Series in the Mississippi River Basin. Remote Sens. 13, 1590. https://doi.org/10.3390/rs13081590

Pavelsky, T.M., Durand, M.T., Andreadis, K.M., Beighley, R.E., Paiva, R.C.D., Allen, G.H., Miller, Z.F., 2014. Assessing the potential global extent of SWOT river discharge observations. J. Hydrol. 519, 1516–1525. https://doi.org/10.1016/j.jhydrol.2014.08.044

Pekel, J.-F., Cottam, A., Gorelick, N., Belward, A.S., 2016. High-resolution mapping of global surface water and its long-term changes. Nature 540, 418–422. https://doi.org/10.1038/nature20584

Ryan, J.C., Smith, L.C., Cooley, S.W., Pitcher, L.H., Pavelsky, T.M., 2020. Global Characterization of Inland Water Reservoirs Using ICESat-2 Altimetry and Climate Reanalysis. Geophys. Res. Lett. 47, e2020GL088543. https://doi.org/10.1029/2020GL088543

Sheng, Y., Song, C., Wang, J., Lyons, E.A., Knox, B.R., Cox, J.S., Gao, F., 2016. Representative lake water extent mapping at continental scales using multi-temporal Landsat-8 imagery. Remote Sens. Environ., Landsat 8 Science Results 185, 129–141. https://doi.org/10.1016/j.rse.2015.12.041

Shiklomanov, A.I., Lammers, R.B., 2009. Record Russian river discharge in 2007 and the limits of analysis. Environ. Res. Lett. 4, 045015. https://doi.org/10.1088/1748-9326/4/4/045015

Smith, L.C., 1997. Satellite remote sensing of river inundation area, stage, and discharge: a review. Hydrol. Process. 11, 1427–1439. https://doi.org/10.1002/(SICI)1099-1085(199708)11:10<1427::AID-HYP473>3.0.CO;2-S

Stan Development Team, 2023. Stan Modeling Language Users Guide and Reference Manual.

Tayfur, G., Moramarco, T., Singh, V.P., 2007. Predicting and forecasting flow discharge at sites receiving significant lateral inflow. Hydrol. Process. 21, 1848–1859. https://doi.org/10.1002/hyp.6320

Tian, W., Liu, X., Wang, K., Bai, P., Liu, C., Liang, X., 2022. Estimation of global reservoir evaporation losses. J. Hydrol. 607, 127524. https://doi.org/10.1016/j.jhydrol.2022.127524

Tuozzolo, S., Lind, G., Overstreet, B., Mangano, J., Fonstad, M., Hagemann, M., Frasson, R.P.M., Larnier, K., Garambois, P.-A., Monnier, J., Durand, M., 2019. Estimating River Discharge With Swath Altimetry: A Proof of Concept Using AirSWOT Observations. Geophys. Res. Lett. 46, 1459–1466. https://doi.org/10.1029/2018GL080771

UNEP, 2016. Transboundary River Basins Status and Trends, Summary for Policy Makers, River Basins. United Nations Environment Programme.

U.S. Geological Survey, 2022. USGS Current Water Data for the Nation [WWW Document]. US Geol. Surv. URL https://waterdata.usgs.gov/nwis/rt (accessed 5.1.21).

Vörösmarty, C.J., Green, P., Salisbury, J., Lammers, R.B., 2000. Global Water Resources: Vulnerability from Climate Change and Population Growth. Science 289, 284–288. https://doi.org/10.1126/science.289.5477.284

Wang, F., Maberly, S.C., Wang, B., Liang, X., 2018. Effects of dams on riverine biogeochemical cycling and ecology. Inland Waters 8, 130–140. https://doi.org/10.1080/20442041.2018.1469335

Wang, J., Sheng, Y., Gleason, C.J., Wada, Y., 2013. Downstream Yangtze River levels impacted by Three Gorges Dam. Environ. Res. Lett. 8, 044012. https://doi.org/10.1088/1748-9326/8/4/044012

Wang, J., Sheng, Y., Wada, Y., 2017. Little impact of the Three Gorges Dam on recent decadal lake decline across China’s Yangtze Plain. Water Resour. Res. 53, 3854–3877. https://doi.org/10.1002/2016WR019817

Wisser, D., Frolking, S., Hagen, S., Bierkens, M.F.P., 2013. Beyond peak reservoir storage? A global estimate of declining water storage capacity in large reservoirs. Water Resour. Res. 49, 5732–5739. https://doi.org/10.1002/wrcr.20452

Yang, T., Zhang, Q., Chen, Y.D., Tao, X., Xu, C., Chen, X., 2008. A spatial assessment of hydrologic alteration caused by dam construction in the middle and lower Yellow River, China. Hydrol. Process. 22, 3829–3843. https://doi.org/10.1002/hyp.6993

Yang, X., Pavelsky, T.M., Ross, M.R.V., Januchowski-Hartley, S.R., Dolan, W., Altenau, E.H., Belanger, M., Byron, D., Durand, M., Van Dusen, I., Galit, H., Jorissen, M., Langhorst, T., Lawton, E., Lynch, R., Mcquillan, K.A., Pawar, S., Whittemore, A., 2022. Mapping Flow-Obstructing Structures on Global Rivers. Water Resour. Res. 58, e2021WR030386. https://doi.org/10.1029/2021WR030386

Yevjevich, V., 1992. Water and Civilization. Water Int. 17, 163–171. https://doi.org/10.1080/02508069208686135

Yoon, Y., Beighley, E., 2015. Simulating streamflow on regulated rivers using characteristic reservoir storage patterns derived from synthetic remote sensing data. Hydrol. Process. 29, 2014–2026. https://doi.org/10.1002/hyp.10342

Yoon, Y., Beighley, E., Lee, H., Pavelsky, T., Allen, G., 2016. Estimating Flood Discharges in Reservoir-Regulated River Basins by Integrating Synthetic SWOT Satellite Observations and Hydrologic Modeling. J. Hydrol. Eng. 21, 05015030. https://doi.org/10.1061/(ASCE)HE.1943-5584.0001320

Zhao, G., Gao, H., 2019. Estimating reservoir evaporation losses for the United States: Fusing remote sensing and modeling approaches. Remote Sens. Environ. 226, 109–124. https://doi.org/10.1016/j.rse.2019.03.015

Zhao, G., Li, Y., Zhou, L., Gao, H., 2022. Evaporative water loss of 1.42 million global lakes. Nat. Commun. 13, 3686. https://doi.org/10.1038/s41467-022-31125-6

Geophysical Research Letters

Supporting Information for

# Turning lakes into river gauges using the LakeFlow algorithm

Ryan M. Riggs[1], George H. Allen[2], Craig B. Brinkerhoff[3], Md. Safat Sikder[4], Jida Wang[4]

(1)Department of Geography, Texas A&M University, College Station, TX, USA, (2)Department of Geosciences, Virginia Polytechnic Institute and State University, Blacksburg, VA, USA, (3)Department of Civil and Environmental Engineering, University of Massachusetts Amherst, Amherst, MA, USA, (4)Department of Geography and Geospatial Sciences, Kansas State University, Manhattan, KS, USA.

**Contents of this file**

Text S1 to S2

Table S1

Figures S1 to S2

## Introduction

This supporting information contains text describing the development of the synthetic dataset and details on the ancillary datasets used in the analysis. In addition, a table of performance metrics is included as well as figures that support the results discussed in the manuscript.

**Text S1: Developing SWOT-like synthetic dataset**

To develop the synthetic SWOT dataset, we leverage gauge records from the USGS (U.S. Geological Survey, 2022), Landsat-based Global Surface Water (GSW) dataset (Pekel et al., 2016), and prior channel attributes in the SWOT River Database (SWORD) (Altenau et al., 2021). For each studied lake, we obtain daily gauge based water volume ($V$) and surface level ($L$) and calculate surface area ($SA$) as

$$SA = dV/dL, \tag{S1}$$

where $dV$ and $dL$ represent daily reservoir volume and level changes, respectively.

To add in SWOT-like errors, we corrupt the surface area ($SA_c$) using 15% relative errors and corrupt water level ($L_c$) using 10-cm error, which corresponds to the mission science requirements of SWOT (Biancamaria et al., 2016). It is worth noting that the error budgets required by the mission science are the expected baseline of SWOT performance, and the actual measurement errors may often be smaller than the science requirement errors applied here (Desrochers et al., 2021). Thus, our LakeFlow assessment using the science requirement error budgets may result in a conservative accuracy. Following this step, we calculate corrupted volume ($V_c$) using

$$V_c = SA_c \times L_c. \tag{S2}$$

For the synthetic river dataset, we rely on the GSW dataset, *in situ* discharge, and SWORD attributes. To produce river width ($W$), we develop a width-discharge power law relationship (Leopold and Maddock, 1953) by pairing minimum width-discharge and maximum width-discharge to develop a linear regression in log-log space. The minimum and maximum discharges are retrieved from the gauge records in our five-year testing period for each lake, whereas the minimum and maximum widths are manually approximated from the GSW water occurrence map assuming the latter can represent river width variability within the testing period. To reduce the possible bias and error in manual approximation, the minimum and maximum widths are further calibrated by the difference between their mean and the channel width recorded in the corresponding SWORD reach. Using this power law relationship, we invert *in situ* discharge to produce a synthetic river width and then we corrupt river width ($W_c$) with 10.6% relative errors (Biancamaria et al., 2016). To produce cross-sectional area changes ($dA$) we assume a simple trapezoidal shape (Tuozzolo et al., 2019) and calculate it as follows:

$$dA = 0.5(W + W_{min}) \times (L - L_{min}), \quad \text{(S3)}$$

where the subscript $min$ denotes the minimum measurement of a parameter. We corrupt cross-sectional area ($dA_c$) using eq. S3, but substituting in the corrupted width ($W_c$) and corrupted level ($L_c$) values. We calculate $A_0$ using eq. 1, where we assume a Manning's n value based on local geology and channel geomorphology (Manning's n values ranging from 0.030 to 0.035 $s/m^{1/3}$) (Brinkerhoff et al., 2020; Chow, 1959; Durand et al., 2014), a slope corresponding to the reach-specific slope value from SWORD, and use the median observed value for the remaining variables. Following this, we consider $A_0$ and $n$ to be constants in time and combine them with the rest of our uncorrupted estimates values in eq. 1 to solve for time varying slope ($S$). We then corrupt slope ($S_c$) using the recommended 1.7 cm/km error (Biancamaria et al., 2016). We limit both the synthetic dataset to one observation each week as SWOT will not provide daily observations. One observation each week is approximately equal to the number of SWOT overpasses for each of our lakes during SWOT's 21-day orbit.

**Text S2: Ancillary data: Lateral inflow data and lake surface evaporation**

For the non-SWOT observed tributary inflow discharge and evaporation, we use modeled daily discharge data from the Global Reach-Level A Priori Discharge Estimates for SWOT

(GRADES) (Lin et al., 2019) and monthly lake surface evaporation estimates from the Global Lake Evaporation Volume (GLEV) dataset (Zhao et al., 2022). GRADES contains daily discharge estimates for 2.94 million river reaches globally from 1979-2014. The discharge is based on runoff simulation from the Variable Infiltration Capacity (VIC) land surface model (Liang et al., 1994), using meteorological forcing that merges gauge-, reanalysis-, and satellite-based data (Beck et al., 2019). The simulated runoff is then routed by the Routing Application for Parallel computation of Discharge (RAPID) model (David et al., 2011) to give discharge for the ~3 million reaches, which offer adequate hydrographic details to represent lateral tributaries to our studied reservoirs. To be consistent with the evaporation dataset, we calculate mean monthly discharge estimates for each reach in GRADES and use these values to estimate a total mean monthly lateral discharge for each reservoir which is denoted as $Q_l$ in eq. 2.

GLEV contains monthly lake evaporation estimates from 1.42 million lakes. GLEV is developed by pairing monthly lake surface area measurements from the Landsat derived GSW dataset (Zhao and Gao, 2018) with monthly meteorological data from several sources (Abatzoglou et al., 2018; Rodell et al., 2004; Xia et al., 2018). Where these meteorological data overlap, the mean monthly value is used to reduce uncertainty. The evaporation rate is then modeled using the Penman Equation (Penman, 1948) with consideration of lake heat storage (Zhao and Gao, 2019). Monthly evaporation loss from each reservoir is calculated as the modeled evaporation rate multiplied by the GSW derived lake surface area and is denoted by $E$ in eq. 2.

**Table S1**. Error metrics used in this study.

| | | |
|---|---|---|
| Nash-Sutcliffe efficiency | $NSE = 1 - \sum_{i=1}^{N}(Q_i - \hat{Q}_i)^2 \,/ \sum_{i=1}^{N}(Q_i - \overline{\mathrm{Q}})^2$ | Where $N$ is the number of timesteps, $Q_i$ is *in situ* discharge at time *i*, $\bar{Q}$ is mean *in situ* discharge, and $\hat{Q}_i$ is LakeFlow estimated discharge at time *i*. |
| Relative bias | $rBias = \frac{1}{N}\sum_{i=1}^{N}\left(\frac{\widehat{Q}_i - Q_i}{Q_i}\right)$ | |
| Normalized root-mean-square error | $NRMSE = \sqrt{\frac{1}{N}\sum_{i=1}^{N}\left(\frac{Q_i - \hat{Q}_i}{\overline{\mathrm{Q}}}\right)^2}$ | |
| Mean absolute error | $MAE = \frac{1}{N}\sum_{i=1}^{N}\left\lvert X_i - \widehat{X}_i\right\rvert$ | Where $N$ is the number of observations, $X_i$ is an *in situ* or synthetic value at time *i* and $\hat{X}_i$ is LakeFlow or SoS estimated value at time *i*. |

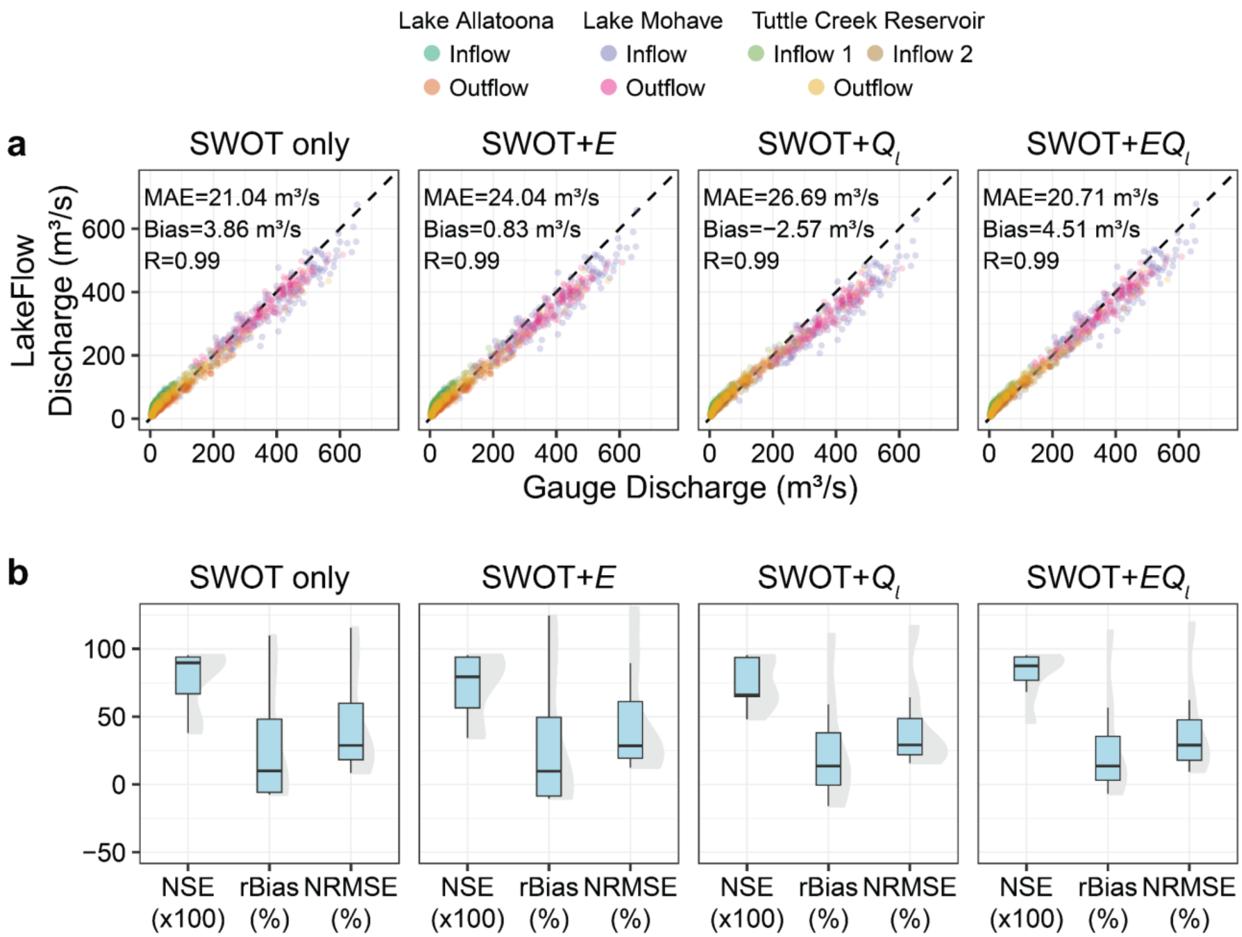


**Figure S1.** LakeFlow discharge performance for four combinations of input data. Synthetic SWOT data with various ancillary data included from no ancillary data ("SWOT only"), only evaporation data ("SWOT+$E$"), only lateral inflow data ("SWOT+$Q_l$"), and both evaporation and lateral inflow data ("SWOT+$EQ_l$"). (a) Scatterplots of same-day gauge discharge vs. LakeFlow estimated discharge across all reaches. (b) Boxplots and half violin plots of LakeFlow discharge performance metrics across all reaches: NSE (scaled by 100), rBias (%), and NRMSE (%).

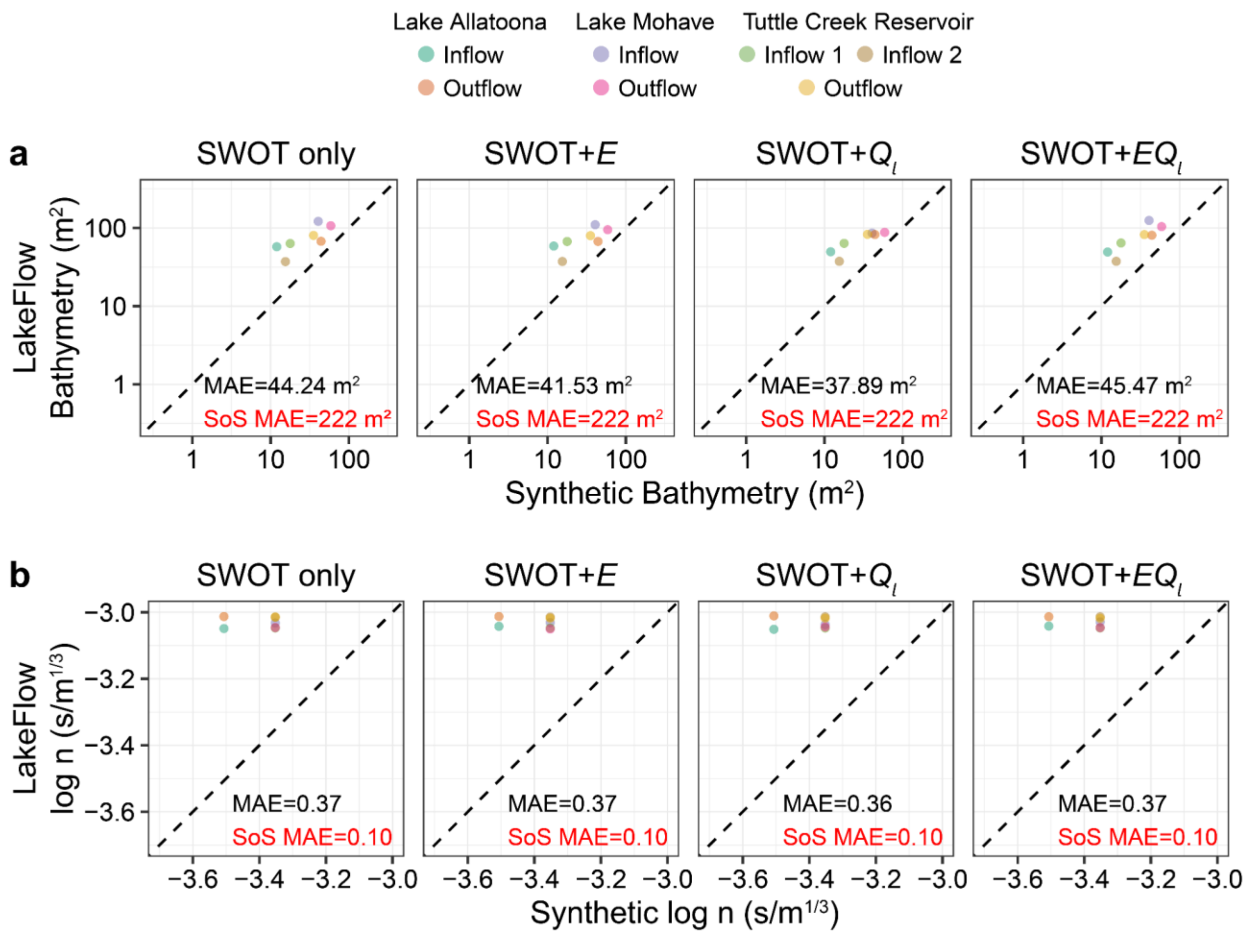


**Figure S2.** The LakeFlow algorithm's performance of unknown variables for four combinations of input data. Synthetic SWOT data with various ancillary data included from no ancillary data ("SWOT only"), only evaporation data ("SWOT+$E$"), only lateral inflow data ("SWOT+$Q_l$"), and both evaporation and lateral inflow data ("SWOT+$EQ_l$"). MAE for LakeFlow (black) and SoS priors (red) shown. (a) Scatterplots of true bathymetry vs. LakeFlow estimated bathymetry across all reaches. (b) Scatterplots of log true Manning's n vs. log LakeFlow estimated Manning's n across all reaches.

## References


Abatzoglou, J.T., Dobrowski, S.Z., Parks, S.A., Hegewisch, K.C., 2018. TerraClimate, a high-resolution global dataset of monthly climate and climatic water balance from 1958–2015. Sci. Data 5, 170191. https://doi.org/10.1038/sdata.2017.191

Altenau, E.H., Pavelsky, T.M., Durand, M.T., Yang, X., Frasson, R.P. de M., Bendezu, L., 2021. The Surface Water and Ocean Topography (SWOT) Mission River Database (SWORD): A Global River Network for Satellite Data Products. Water Resour. Res. 57, e2021WR030054. https://doi.org/10.1029/2021WR030054

Beck, H.E., Wood, E.F., Pan, M., Fisher, C.K., Miralles, D.G., van Dijk, A.I.J.M., McVicar, T.R., Adler, R.F., 2019. MSWEP V2 Global 3-Hourly 0.1° Precipitation: Methodology and Quantitative Assessment. Bull. Am. Meteorol. Soc. 100, 473–500. https://doi.org/10.1175/BAMS-D-17-0138.1

Biancamaria, S., Lettenmaier, D.P., Pavelsky, T.M., 2016. The SWOT Mission and Its Capabilities for Land Hydrology. Surv. Geophys. 37, 307–337. https://doi.org/10.1007/s10712-015-9346-y

Brinkerhoff, C.B., Gleason, C.J., Feng, D., Lin, P., 2020. Constraining Remote River Discharge Estimation Using Reach-Scale Geomorphology. Water Resour. Res. 56, e2020WR027949. https://doi.org/10.1029/2020WR027949

Chow, V.T., 1959. Open-channel hydraulics. McGraw-Hill, New York.

David, C.H., Maidment, D.R., Niu, G.-Y., Yang, Z.-L., Habets, F., Eijkhout, V., 2011. River Network Routing on the NHDPlus Dataset. J. Hydrometeorol. 12, 913–934. https://doi.org/10.1175/2011JHM1345.1

Desrochers, N.M., Trudel, M., Biancamaria, S., Siles, G., Desroches, D., Carbonne, D., Leconte, R., 2021. Effects of Aquatic and Emergent Riparian Vegetation on SWOT Mission Capability in Detecting Surface Water Extent. IEEE J. Sel. Top. Appl. Earth Obs. Remote Sens. 14, 12467–12478. https://doi.org/10.1109/JSTARS.2021.3128133

Durand, M., Neal, J., Rodríguez, E., Andreadis, K.M., Smith, L.C., Yoon, Y., 2014. Estimating reach-averaged discharge for the River Severn from measurements of river water surface elevation and slope. J. Hydrol. 511, 92–104. https://doi.org/10.1016/j.jhydrol.2013.12.050

Leopold, L.B., Maddock, T., 1953. The Hydraulic Geometry of Stream Channels and Some Physiographic Implications. U.S. Government Printing Office.

Liang, X., Lettenmaier, D.P., Wood, E.F., Burges, S.J., 1994. A simple hydrologically based model of land surface water and energy fluxes for general circulation models. J. Geophys. Res. Atmospheres 99, 14415–14428. https://doi.org/10.1029/94JD00483

Lin, P., Pan, M., Beck, H.E., Yang, Y., Yamazaki, D., Frasson, R., David, C.H., Durand, M., Pavelsky, T.M., Allen, G.H., Gleason, C.J., Wood, E.F., 2019. Global Reconstruction of Naturalized River Flows at 2.94 Million Reaches. Water Resour. Res. 55, 6499–6516. https://doi.org/10.1029/2019WR025287

Pekel, J.-F., Cottam, A., Gorelick, N., Belward, A.S., 2016. High-resolution mapping of global surface water and its long-term changes. Nature 540, 418–422. https://doi.org/10.1038/nature20584

Penman, H.L., 1948. Natural evaporation from open water, bare soil and grass. Proc. R. Soc. Lond. Ser. Math. Phys. Sci. 193, 120–145. https://doi.org/10.1098/rspa.1948.0037

Rodell, M., Houser, P.R., Jambor, U., Gottschalck, J., Mitchell, K., Meng, C.-J., Arsenault, K., Cosgrove, B., Radakovich, J., Bosilovich, M., Entin, J.K., Walker, J.P., Lohmann, D., Toll, D., 2004. The Global Land Data Assimilation System. Bull. Am. Meteorol. Soc. 85, 381–394. https://doi.org/10.1175/BAMS-85-3-381

Tuozzolo, S., Langhorst, T., de Moraes Frasson, R.P., Pavelsky, T., Durand, M., Schobelock, J.J., 2019. The impact of reach averaging Manning's equation for an in-situ dataset of water surface elevation, width, and slope. J. Hydrol. 578, 123866. https://doi.org/10.1016/j.jhydrol.2019.06.038

U.S. Geological Survey, 2022. USGS Current Water Data for the Nation [WWW Document]. US Geol. Surv. URL https://waterdata.usgs.gov/nwis/rt (accessed 5.1.21).

Xia, X., Zhang, S., Li, S., Zhang, Liwei, Wang, G., Zhang, Ling, Wang, J., Li, Z., 2018. The cycle of nitrogen in river systems: sources, transformation, and flux. Environ. Sci. Process. Impacts 20, 863–891. https://doi.org/10.1039/C8EM00042E

Zhao, G., Gao, H., 2018. Automatic Correction of Contaminated Images for Assessment of Reservoir Surface Area Dynamics. Geophys. Res. Lett. 45, 6092–6099. https://doi.org/10.1029/2018GL078343

Zhao, G., Li, Y., Zhou, L., Gao, H., 2022. Evaporative water loss of 1.42 million global lakes. Nat. Commun. 13, 3686. https://doi.org/10.1038/s41467-022-31125-6